CANADIAN THESES

THÈSES CANADIENNES

NOTICE

The quality of this microfiche is heavily dependent upon the quality of the original thesis submitted for microfilming. Every effort has been made to ensure the highest quality of reproduction possible.

If pages are missing, contact the university which granted the degree.

Some pages may have indistinct print especially if the original pages were typed with a poor typewriter ribbon or if the university sent us an inferior photocopy.

Previously copyrighted materials (journal articles, published tests, etc.) are not filmed.

Reproduction in full or in part of this film is governed by the Canadian Copyright Act, R.S.C. 1970, c. C-30.

AVIS

La qualité de cette microfiche dépend grandement de la qualité de la thèse soumise au microfilmage. Nous avons tout fait pour assurer une qualité supérieure de reproduction.

S'il manque des pages, veuillez communiquer avec l'université qui a conféré le grade.

La qualité d'impression de certaines pages peut laisser à désirer, surtout si les pages originales ont été dactylographiées à l'aide d'un ruban usé ou si l'université nous a fait parvenir une photocopie de qualité inférieure.

Les documents qui font déjà l'objet d'un droit d'auteur (articles de revue, examens publiés, etc.) ne sont pas microfilmés.

La reproduction, même partielle, de ce microfilm est soumise à la Loi canadienne sur le droit d'auteur, SRC 1970, c. C-30.

THIS DISSERTATION HAS BEEN MICROFILMED EXACTLY AS RECEIVED

LA THÈSE A ÉTÉ MICROFILMÉE TELLE QUE NOUS L'AVONS REÇUE

Tests and Strength Evaluation of Composite Fibre Reinforced Panels (Bumaco Laminated Panels)

M. A. Rohadi

A Thesis

in

the Department

of

Civil Engineering

Presented in Partial Fulfillment of the Requirements
for the Degree of Master of Engineering at
Concordia University
Montréal, Québec, Canada

March 1986

ISBN 0-315-30602-5

ABSTRACT

Tests and Strength Evaluation of Composite Fibre Reinforced Panels

M. A. Rohadi

Tests and evaluations of the flexural strength and compressive bearing capacity of new composite panels designed for cladding walls and for the construction of terraces are presented in this thesis. These new composite panels are the product of lamination of marble conglomerate or solid granite and asbestos - cement densite. Asbestos - cement serves as the main reinforcing material.

Full scale composite panels were tested as simply supported beams and slabs, and as bearing walls subjected to axial compression. Additional tests were performed for racking and impact loads.

The analysis method for evaluating the flexural capacity of these composite panels was developed based on the non - linear stress distribution at cracking. Calculated results were then compared with test values. The application of the modified empirical ACI formula (section 14.2.3 of ACI 318 - 83) for concrete walls was verified for walls made of these new panels.

ACKNOWLEDGEMENTS

This research was carried out based on a contract agreement with Atlas Turner Inc. and Bumaco (Building Materials Corp.), and special thanks go to them for producing and preparing the test panels used in this research project.

The author wishes to express his sincere gratitude to Dr. Z. A. Zielinski, project director, for his guidance, cooperation and encouragement throughout all stages of this research program and the preparation of this thesis.

Special acknowledgements are also extended to my colleague Mr. Alan K. Yep for his participation and help during the experimental program, and also for his excellent job in typing this thesis.

Thanks are also due to Concordia University for the use of the structural laboratory and to the technicians D. Roy and L. Stankevicious for their assistance.

Last, but not least, the author would like to thank his mother, Mrs. A. R. Roekjat for her infinite patience and understanding.

TABLE OF CONTENTS

LIST OF FIGURES

LIST OF TABLES

NOMENCLATURE

A_s	Area of tension reinforcement
A'_s	Area of compression reinforcement
ΔA_c	Area of asbestos - cement in tension in excess of basic rectangular section (bh)
$\Delta A'_c$	Area of asbestos - cement in compression in excess of basic rectangular section (bh)
b	Width of basic rectangular section, as defined in Figure 4.3 (a)
E_s	Modulus of elasticity of steel
ε_{cc}	Strain at the extreme compression fibre of asbestos - cement section
ε_{ct}	Maximum strain at the extreme tension fibre of asbestos - cement section
f_{ci}	Compressive stress in asbestos - cement section corresponding to $\Delta A'_c$
f_{cc}	Compressive stress at the extreme compression fibre of asbestos - cement section, as defined in Figure 4.3 (c)
f'_s	Stress in the compression reinforcement, as defined in Figure 4.3 (c)
f_s	29.0 ksi, stress in tension reinforcement at cracking stage assuming that strain in tensioned asbestos - cement is 0.001
f_{to}	Flexural tensile strength of asbestos - cement
f_{tm}	Flexural tensile strength of marble conglomerate
f_{tol}	Flexural tensile strength of asbestos - cement in the longitudinal direction
f_{tot}	Flexural tensile strength of asbestos - cement in the transverse direction
σ_{Lult}	Ultimate direct tensile strength of asbestos - cement in the longitudinal direction
d''	Compression steel cover
d_s	Tension steel cover
d_Δ	Distance from the extreme tension fibre to the centre of gravity of ΔA_c
d_o	Distance from the extreme tension fibre to the centre of gravity of the basic rectangular section below the neutral axis

d'_s	Distance between compression steel and tension steel
x	Distance from neutral axis to the extreme compressive fibre
n	Steel and asbestos - cement modular ratio (E_s/E_c)
h	Overall depth of basic rectangular section, as defined in Figure 4.3 (a)
h_d	Thickness of asbestos - cement layer in veneer specimen, as defined in Figure 4.5 (a)
h_m	Thickness of marble slab in veneer panels, as defined in Figure 4.5 (a)
h_g	Thickness of granite slab in granite pavers, as defined in Figure 4.6 (a)
h_{d1}	Thickness of the first asbestos - cement layer in granite pavers, as defined in Figure 4.6 (a)
h_{d2}	Thickness of the second asbestos - cement layer in granite pavers, as defined in Figure 4.6 (a)
d_{asb}	Distance from the extreme tension fibre to the centroid of asbestos - cement area in veneer panels, as defined in Figure 4.5 (d)
d'_{asb}	Distance from the extreme tension fibre to the centroid of the upper asbestos - cement layer in veneer panels, in granite layers, as defined in Figure 4.5 (d)
T_{asb}	The tensile force contribution of asbestos - cement layer in veneer panels
T'_{asb}	The tensile force contribution of the upper (first) asbestos - cement layer in granite panels
ε_{cme}	Strain in the extreme compression fibre of marble, during elastic stage
ε_{tae}	Strain in the extreme compression fibre of asbestos - cement, during elastic stage
f_{cme}	Compressive stress in the extreme compression fibre of marble, during elastic stage
f_{cae}	Compressive stress in the extreme compression fibre of asbestos - cement, during elastic stage
f_{tae}	Tensile stress in the extreme tension fibre of asbestos - cement, during elastic stage

M_{cr}	The ultimate (cracking) moment
ϕ	Capacity reduction factor
ψ_c	Coefficient of strengthening of section in compression in excess of basic rectangular section
ψ_t	Coefficient of strengthening of section in tension in excess of basic rectangular section
$\sigma, \Sigma\psi_{ti}\delta_i$	Terms defined by equation (4.8)
w_l	Uniform linear failure load
w	Failure load per unit area
w_{uv}	Ultimate failure load on veneer panels in bending
w_{avd}	Allowable load on veneer panels under dry conditions
w_{avw}	Allowable load on veneer panels under wet conditions
w_{up}	Ultimate failure load on granite pavers in bending
w_{apd}	Allowable load on granite pavers under dry conditions
w_{apw}	Allowable load on granite pavers under wet conditions
P_u	Ultimate bearing capacity of wall
P_n	Nominal bearing capacity of wall
f'_c	Specified compressive strength of concrete
f_{cm}	Specified compressive strength of marble
f_{ca}	Specified compressive strength of asbestos - cement
k	Effective length factor
l_e	Critical length between supports
A_g	Gross area of section
A_m	Gross area of marble layer
A_{asb}	Gross area of asbestos - cement layer
m	Ratio of f_{ca} to f_{cm} (f_{ca}/f_{cm})
ρ	Ratio of A_{asb} to A_m (A_{asb}/A_m)

f'_t Direct tensile strength of concrete

f_a Average tensile stress of concrete

CHAPTER I

INTRODUCTION

1.1 General

Stone products are used mainly for architectural cladding and paving (granite, marble and travertine). However, regular stone products are generally too heavy, brittle and expensive. Due to these drawbacks, architects/designers hesitate to use natural stone products as the main components for establishing the intended aesthetic appearance of a building.

Natural stone products which are commonly used in building construction have certain setbacks which can be summarized as follows:

1. the conventional natural stone products are generally heavy and require delicate handling. In addition, they can only be delivered in small segments; and
2. connection details are difficult to standardize due to varying structural conditions as this will result in high cost of erection, and therefore be uneconomical.

In an attempt to overcome the above disadvantages, Atlas Turner Inc. and Bumaco Inc., both of Montreal, introduced a new laminated composite stone panel. This new product is a sandwich of a thin stone slab and asbestos - cement which has several distinct advantages including:

1. the architects/designers can use natural stone products as large size panels for wall claddings and pavings, floors and plaza surfacing due to the increased flexural strengths;
2. the composite stone panels are good for energy conservation;
3. the cost savings on installation and transportation can be achieved due to the large size and smaller thicknesses of the composite panels; and
4. the composite stone panels are durable and maintenance free.

1.2 Scope of the Study

The development of the Bumaco composite panels was undertaken based on the strength advantages of asbestos - cement. The main purpose of this research program is to define the strength properties of the Bumaco composite panels and to provide the required design guidelines. The research program is based on both an experimental and theoretical investigation.

The experimental program includes full - scale tests on composite panels made of marble and granite to define strength in service condition, and small - scale samples to define the strength characteristics of composite materials. The test results are meant to provide for a basis for verification of the analytical techniques.

The theoretical study program is directed towards the development of design formulae and recommendations for applications for composite panels which may be subjected to flexural and compressive loadings.

CHAPTER II

DESCRIPTION OF BUMACO SYSTEM

2.1 Bumaco Veneer Panels

Veneer panels are the product of lamination of two materials, namely a stone slab of solid granite or marble or marble conglomerate and asbestos - cement (densite). The facing material (1/2" stone slab) and a 3/8" densite sheet are glued together under pressure with epoxy resin produced by the Sika Corporation.

Two marble conglomerates, one made of a dark green marble named 'Verde Polcevera' (designated as Type I marble) and the other of a white marble (designated as type II marble), were tested. These marble types were produced as a conglomerate of marble aggregate and a special synthetic resins by Adige Marmoresina of Italy.

Bumaco veneer panels may have various applications in the construction of a building, which include:

1. Veneer panels for lobby walls in old or new construction. They can be installed directly to stud walls replacing gypsum boards which have been used traditionally. If walls of brick, block or concrete are existing, veneer panels can be fastened by drilling through the face of the panel and installing threaded masonry screws of high strength alloy steel. Screw heads can then be concealed with the use of coloured epoxy to match the veneer (see Figure 2.1).
2. Veneer panels may be used as one of the components for the "s" panels shown in Figure 2.2. The "s" panel is fabricated by coating the apex of each corrugation on the asbestos - cement (densite) core with a gel type epoxy. A 3/8" flat asbestos - cement sheet (densite) is then placed on top of the epoxied core and the two sheets are riveted together. The panel is then reversed and the process is repeated to

complete the base panel. The preassembled panel is then brought to a laminating station where the epoxy and finish facing (marble or other stones) are applied and subjected to pressure on hydraulically activated tables. Following a curing period, the laminated panels can be sawed and modified to special shapes as required by design. The "s" panel cores can then be injected with polyurethane foam insulation (approximate "R" value of 15). Various anchor assemblies may be adapted to suit suspension systems.

2.2 Bumaco Granite Pavers

Granite pavers are the product of lamination of solid granite slabs and two layers of asbestos - cement densite sheets. The 3/8" densite sheets are glued together with epoxy resins with their fibre directions oriented perpendicular to each other. This combined sheet and 1" granite slab are then laminated under pressure with the same epoxy resin. The tested pavers were produced using grey granite from St. Gerard, Quebec.

The granite pavers are used mainly as an architectural cover for the construction of terraces and plazas which are supported at four corners. The laminated panels may be used as square slabs or modified to special shapes and geometric patterns which will suit the span length between supports.

2.3 Material Properties

The mechanical properties of asbestos - cement sheet (densite), granite and marble are given in Table 2.1 in accordance with the specifications of Atlas Turner and Bumaco.

The stress-strain curve for asbestos - cement 'densite' was obtained from the direct tensile test done by Perinayegon [7], and which is shown in Figure 2.3. The modulus of elasticity of 'densite' was also found to be $E = 1.75 \times 10^6$ psi and the ultimate direct tensile strength 1900 psi. Samples were tested with their fibre orientation being

parallel to the tension direction.

Material Properties		Asbestos-cement (densite)	Granite (Vert St-Gerard)	Marble (verde polcevera)
Modulus of Rupture (lb./sq. in)	Along fibers	4500	2442	2045
	Across fibers	3700		
Uniaxial tensile Strength (lb./sq. in)	Along fibers	2220	1395	1160
	Across fibers	1450		
Compressive strength (lb./sq. in)		12500	22915	16795

Table 2.1: Mechanical properties of materials used for producing Bumaco composite panels as specified by Atlas Turner Inc. and Bumaco.

Notes:

- modulus of rupture, flexural strength and compressive strength of natural building stone were obtained based on ASTM Specifications number C99, C880 and C170 respectively; and
- mechanical properties of asbestos - cement densite were defined according to the ASTM specifications number C220 - 75.
- the uniaxial tensile strength of marble conglomerate was defined by dividing the modulus of rupture (obtained in accordance to ASTM Standard C99) by a factor of 1.75. The factor of 1.75 is used based on literatures [10, 11].

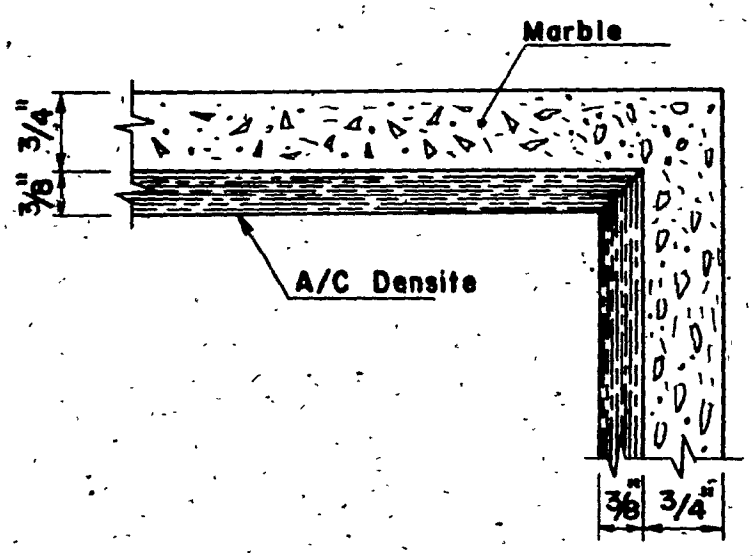

Figure 2.1 Typical application of veneer panels in lobby walls

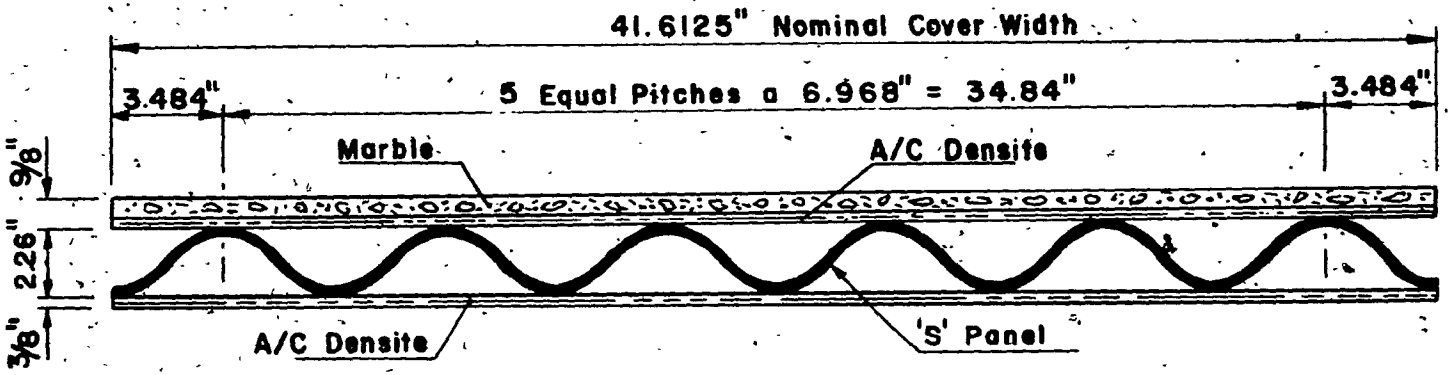

Figure 2.2 Veneer panels on A/C 'S' panel

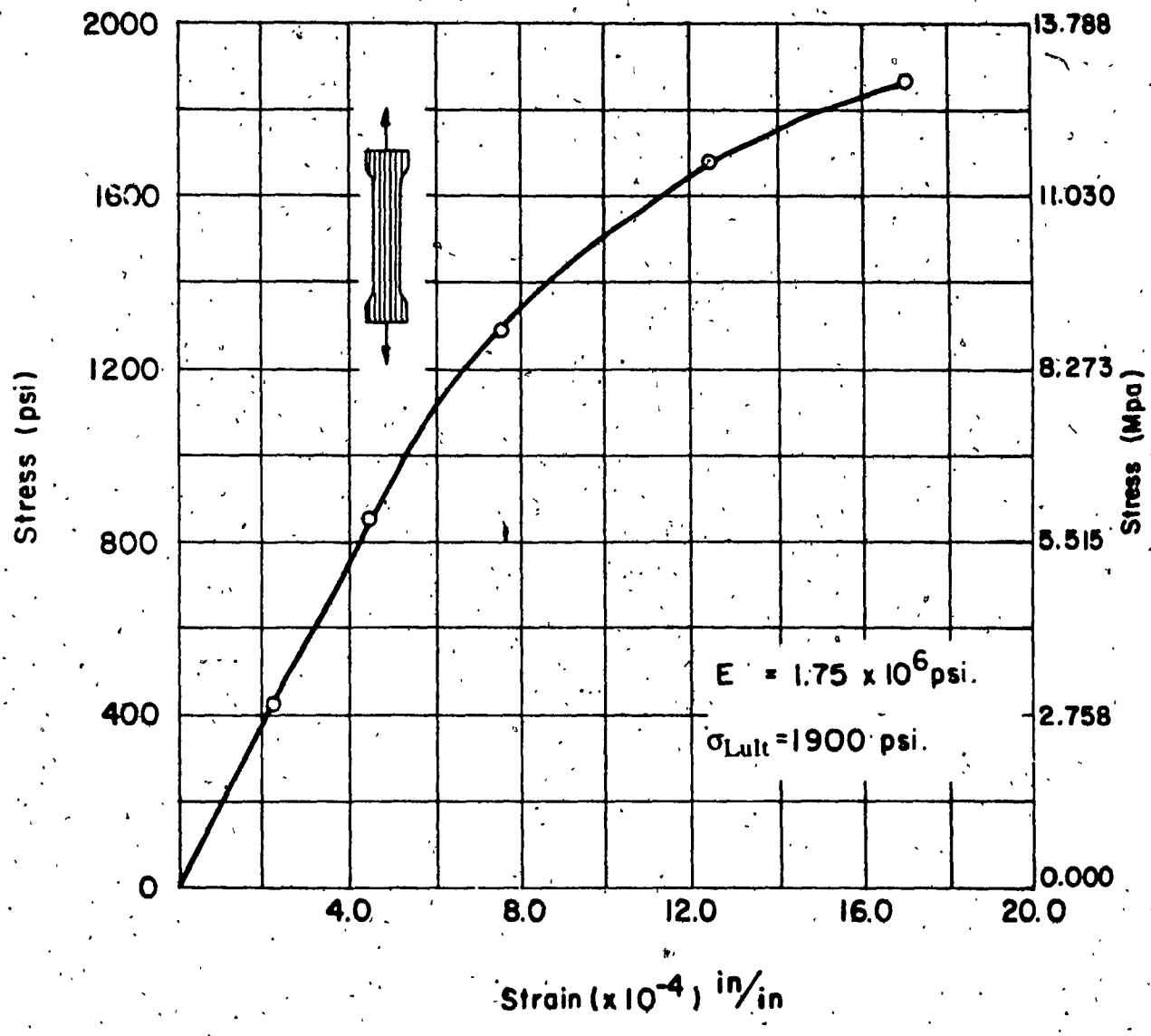

Figure 2.3 Stress-strain curve for asbestos-cement in tension along the fibres

CHAPTER III

EXPERIMENTAL PROGRAM AND RESULTS

3.1 Introduction

Testing of full - scale Bumaco laminated panels is of major interest to the present study arising from the fact that full - scale testing is the most reliable means of obtaining real performance data by which the importance of the different analytical techniques can be judged.

Standard ASTM test methods [1, 2, 3] were used in this study whenever they were applicable. Procedures and results of each of the tests performed are described in the following sections.

3.2 Test Specimens

A total of five veneer panels of 23" x 114" x 7/8" size were used for flexural tests. Two of the above panels were composed of the dark green 'Verde polcevera' marble conglomerate and three of the white 'Carrare veine c' marble conglomerate. Additional tests were performed on three 37" x 39" x 2" granite paver specimens. Detailed descriptions of these test series are given in Tables 3.1 and 3.2 respectively.

To determine the compressive strength of veneer panels, two 23" x 114" x 7/8" veneer specimens containing white 'carrare veine c' marble were tested. Racking as well as impact loading tests were performed on the veneer specimens. The detailed dimensions are shown in Table 3.3.

3.3 Flexural Tests on Veneer and Granite Paver Specimens

3.3.1 Testing Procedures

Flexural tests on veneer panels consisted of two phases. The first phase was to test veneer panels as a simply supported beam under a uniformly distributed load and with densite sheet located at the bottom (tension) face (test series BMC1-BMC2/TPI and BMC1-BMC /TPII). Panel was rested on roller supports consisting of 1/4" steel plates and steel pipes of 1" diameter. The testing arrangements are shown in Figures 3.1 and 3.2. Once the panel was installed and ready for testing, dial gauges were placed and adjusted. A uniformly distributed load was gradually applied by means of 10 lb sand bags placed on top of the panel in a prescribed order. The deflection and load readings were taken in increments of 50 lbs. The panel was allowed to stabilize for 2 minutes before any readings were recorded. This loading was continued until the ultimate capacity was reached. At failure, crack patterns as well as failure load were marked on the panel and photographs were taken.

The second phase involved the testing of cut-out portions of veneer panels used in the first phase. These portions were cut from areas where the material was not under maximum stress during first phase testing nor injured. Their span length varied from 38 inches to 57 inches. The same roller supports were used as in the first phase, but with different loading arrangements. In test series BMCN1-BMCN3 and BMCR1-BMCR3 of both types I and II marble respectively, loads were applied at a distance of 0.25L from both supports by means of cross beams attached to two hydraulic jacks, and with load increments of 47.5 lbs. In the second set-up test series BMSN1-BMSN3 and BMSR1 of type II marble, loads were applied at midspan through a single cross beam connected to a hydraulic jack at the center. Deflection and load readings were taken at an increment of 47.5 lbs. In both cases, samples were tested with densite sheets located at the top surface of the panel (BMCR and BMSR series) and bottom surface (BMCN and BMCR series). Both loading arrangements are shown in Figures 3.3 and 3.4 respectively.

Granite paver specimens were tested as two way four point loaded slabs, placed on four corners on supporting pads with densite sheet on the bottom tension side (test series 1-GP1 and 1-GP3). Each supporting pad was made of two 4" x 4" x 3/4" neoprene. The loads were applied by means of two cross beams attached to a main loading beam which in turn was connected to a single hydraulic jack at the center (Figure 3.5). This loading arrangement was intended to simulate a uniform load. Dial gauges were used to measure deflections. Deflection readings were recorded at a load increment of 2,375 lbs. Failure modes and crack patterns were noted and photographed.

3.3.2 Test Results

For the test series BMC1-BMC2 of type I marble and BMC1-BMC3 of type II marble, all the specimens failed suddenly (broke into two pieces) when a tension crack appeared in the vicinity of the midspan (see Figures 3.6 and 3.7). It was also observed that veneer panels lost their flexural resistance as soon as the asbestos-cement sheet ruptured. However, no crushing of marble stone was found at the compression zone. The ultimate loads for panels BMC1 and BMC2 type I were 300 lbs and 320 lbs respectively, while panels BMC1-BMC3 type II failed under the loads of 520 lbs, 450 lbs and 390 lbs respectively. Corresponding equivalent uniformly distributed loads were calculated as shown in Table 3.4. The load deflection curves for these test series are shown in Figures 3.8 and 3.9.

In test series BMCN1-BMCN3 of type I marble, the three specimens failed by a sudden tension crack in the area between the two loading beams (Figure 3.10). The same failure mode was observed in test series BMCR1-BMCR3 of type I and type II marble (Figures 3.11 and 3.12), but the failure loads were much lower than the ones obtained in test series BMCN. This proved that asbestos - cement increased the flexural strength of ordinary marble stone panels. A summary of experimental results was shown in Tables 3.5 and 3.6 load deflection curves for the panels were shown in Figures 3.13 and 3.14.

All panels in test series BMSN1-BMSN3 and BMSR1-BMSR3 of type II marble failed directly under the point of load application, by tearing apart in the tension zone. It was again noticed that failure loads obtained from test series BMSR were much lower than results obtained from BMSN. Test results were summarized in Tables 3.7 and 3.8 while Figures 3.15 and 3.16 show the load deflection curves of the tested panels.

Test results on granite pavers are illustrated in Figures 3.17 and 3.18. Failure due to a sudden tension crack in the region between the two cross-beams was observed in all granite paver specimens (see Figure 3.17) except for specimen 1-GP3 where cracks were radiated from P1 to L2 and to the adjacent edges (Figure 3.18). The test results are given in Table 3.9.

Additional tests were performed on broken pieces saved from test series 1-GP. In these tests, samples were tested as one way beams, and placed on rolling supports, with granite on the bottom tension side. Two loads were applied by means of two cross-beams and main beam which was attached to the Tinus-Olsen loading machine as shown in Figure 3.19. All specimens failed when crack appeared between the two loading beams. Test results are shown in Table 3.10.

3.4 Compression Tests on Veneer Panels

3.4.1 Testing Procedures

Compression tests were performed on two veneer panels (BMW1 and BMW2 of type II marble) in a special frame shown in Figure 3.20. The set-up consisted of an overhead mounted hydraulic jack connected to a rigid steel beam. Panels were braced at front and back faces by 2" x 4" pieces of wood. Bracing locations were shown in Figure 3.20. Dial gages were used to measure panel displacements and were placed near the bracing woods and at the center line between two braces (Figure 3.20). Loads were then exerted gradually in equal increments of 1,180 lbs until the ultimate capacity was reached.

3.4.2 Tests Results

All panels showed a similar mode of behaviour. Failure occurred suddenly in the region between two braces. The average failure load of the two panels tested was 20.58 kips. The experimental results were tabulated in Table 3.11. The horizontal displacement of center points of panels BMW1 and BMW2 (nodes CT and CB) are illustrated in Figure 3.21. The mode of displacement, prior to failure, is shown in Figure 3.22.

3.5 Racking Tests on Veneer Panels

3.5.1 Testing Procedures

The apparatus for the simulated racking tests were assembled as shown in Figure 3.23 and 3.24. The test panel was positioned in such a way that its diagonal was perpendicular to the base of the testing machine. In the case of test panel BMR2, wood bracings were provided at a distance of 30.5 inches from the base (Figure 3.24). Load was applied to the specimen through steel saddles which were specially designed to accomodate the test panel. The steel saddles were securely bolted to the base and top of the testing machine. Electric strain gauges (type EA-06-20 CBW-120, manufactured by Micro - Measurement) were provided at the locations, as shown in Figure 3.23 and 3.24, to measure the compressive strains along the diagonal and the tensile strains across the diagonal. The load was applied continuously throughout test at a uniform rate until failure. Displacement readings were recorded at load increments of 1,000 lbs. The behavior of the panel during the test and at failure was carefully observed. Any visible failure from loading was marked and photographed.

3.5.2 Test Results

For the unbraced veneer specimens, failure was caused by buckling across the vertical diagonal as shown in Figure 3.25. The maximum load at which buckling occurred was 19.975 kips. For braced veneer specimens, failure was caused by splitting along the vertical diagonal as shown in Figure 3.26. The maximum load at which splitting took

place was 49.4 kips.

3.6 Impact Tests on Veneer Panels

3.6.1 Testing Procedures

Standard ASTM test methods [2, 3] are employed in impact tests. The purpose of this test was to provide data that can be used to evaluate the relative performance of wall and floor constructions under conditions representative of those sustained in actual service when subjected to impact by a heavy blunt object.

The specimen was tested as shown in Figure 3.27, as a simple beam on a span of 48 inches. The two roller supports were designed to prevent longitudinal restraint and provide bearing for the entire width of the specimen. The ends of the panel were secured by hold-downs to minimize specimen bounce. Special care was taken to assure that the hold-downs did not affect deflection of the specimen. An impact load was then applied to the upper face of the specimen by dropping the 50 lb sand bag beginning with a height of 6 inches (152 mm) and increasing the height by 6 inch increments. Instantaneous deflection measurements were recorded for each drop by means of two displacement transducers attached to the midspan edges of the panel. For the first drop, the height of the bag was measured from the upper face of the specimen at a point directly beneath the bag, and for subsequent drops, from a taut cord in contact with the upper face vertically above the supports. The impact test was continued until the specimen could no longer support the 50 pound load.

3.6.2 Test Results

The recorded maximum drop height at which the veneer specimens broke in half was 66 inches. No significant damage prior to this maximum drop height was observed on the specimen. Instantaneous deflections were plotted against the drop height and is shown in Figure 3.28.

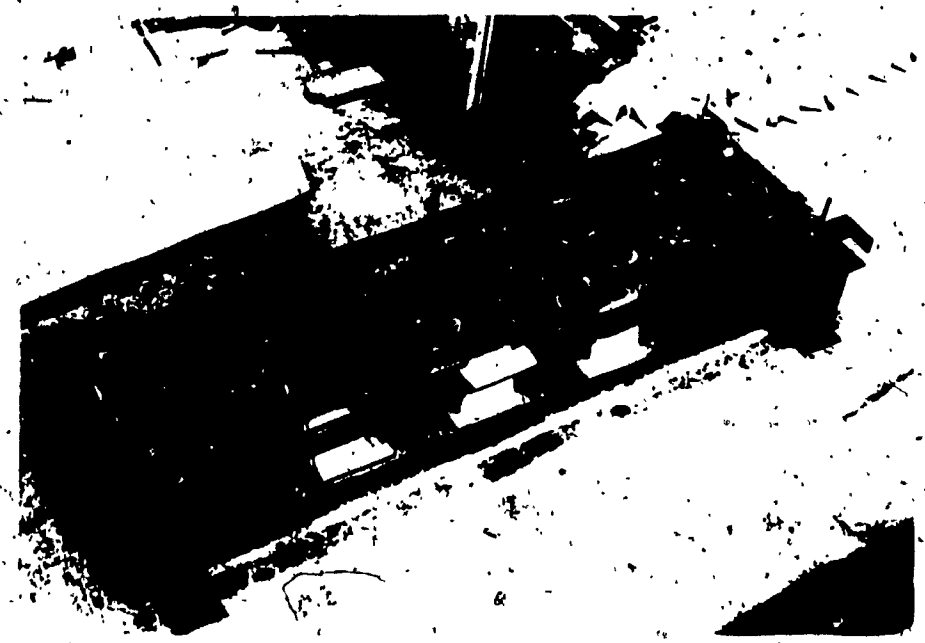

Figure 3.1 View of testing arrangement for uniform load (before loading)

Figure 3.2 View of testing arrangement for uniform load (during loading)

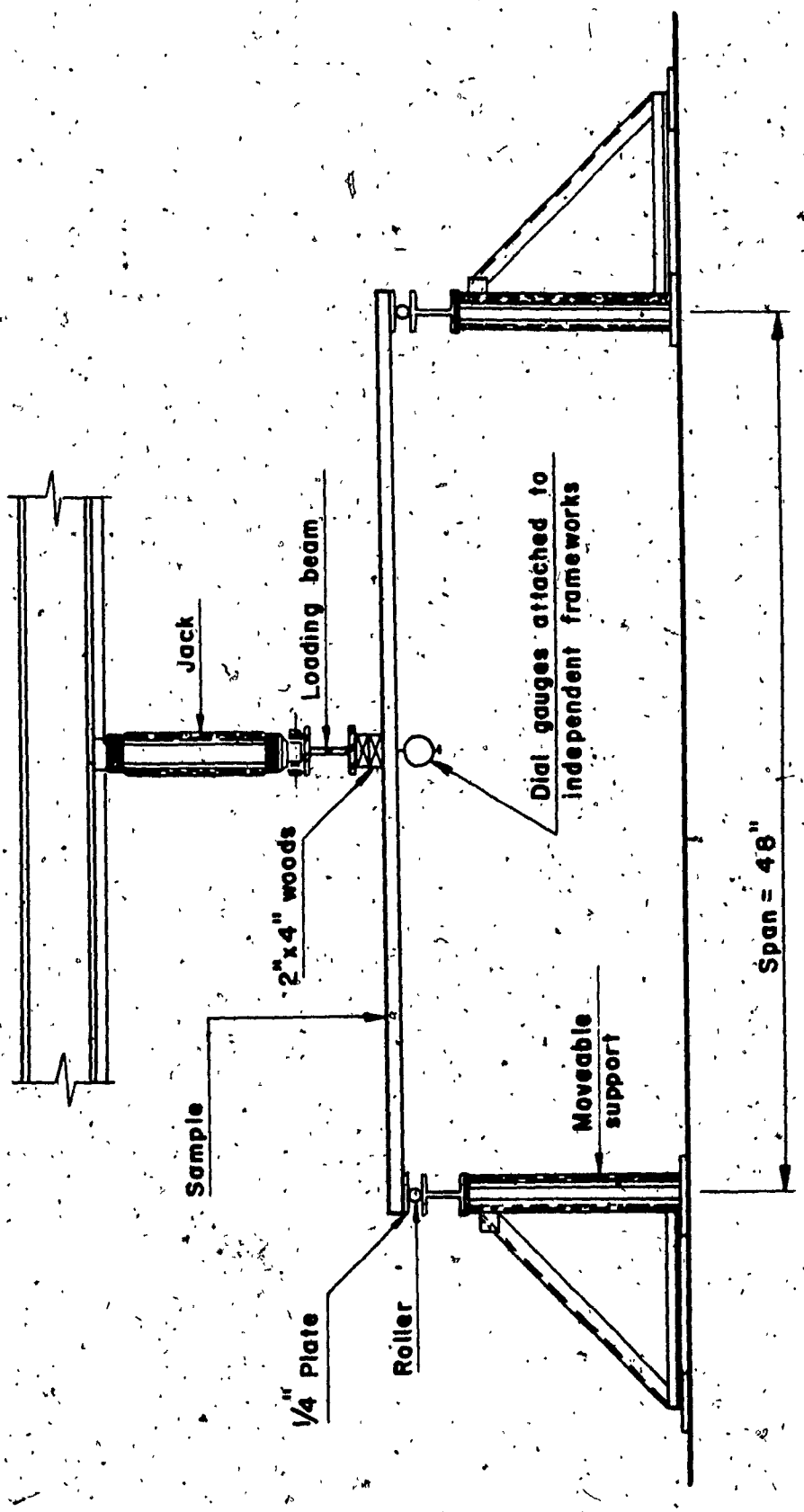

Figure 3.3 Testing arrangement for half span loading

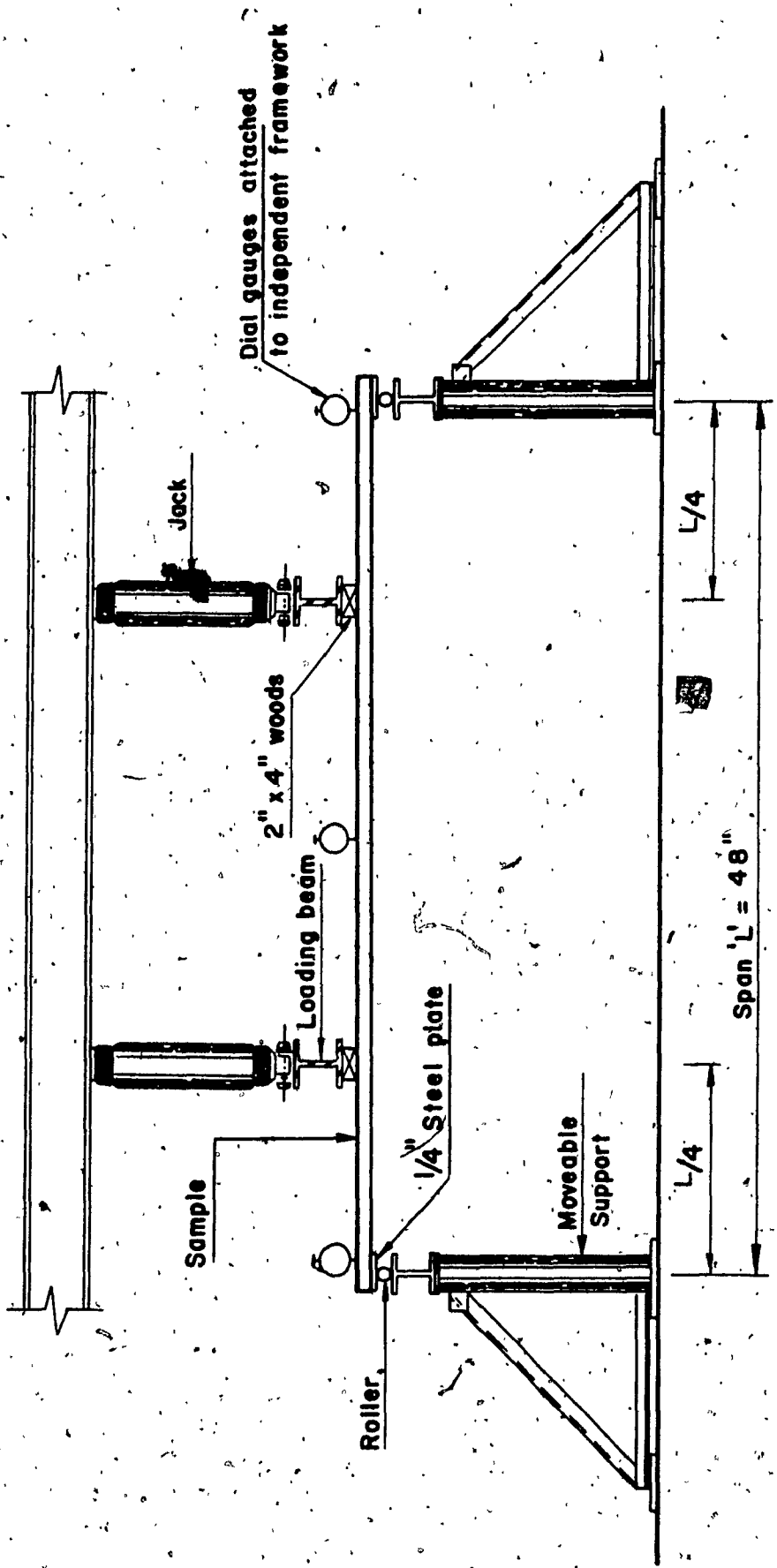

Figure 3.4 : Testing arrangement for quarter-span loading

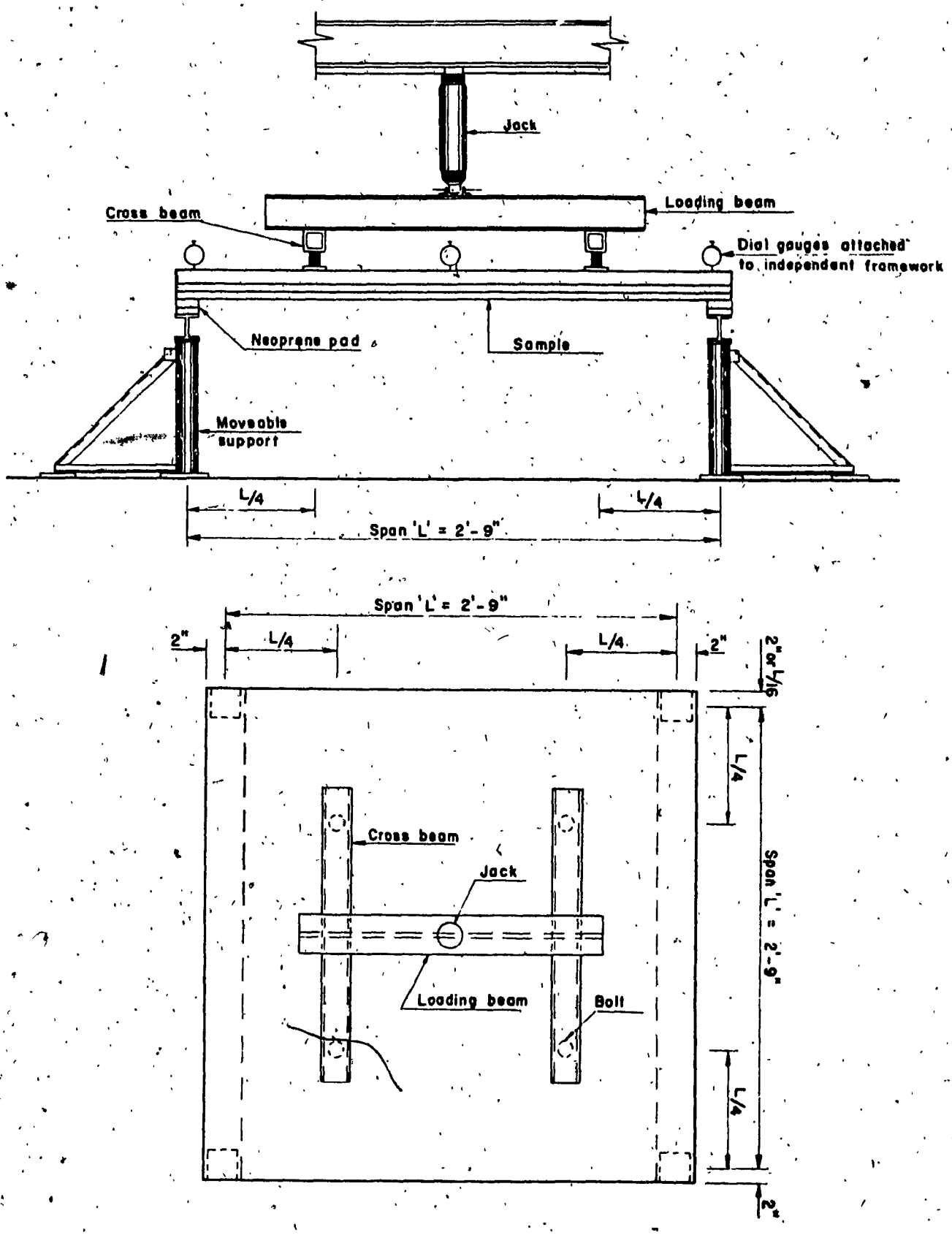

Figure 3.5 Testing arrangement for granite pavers: (a) side view; (b) plan view

Figure 3.6 Typical view of BMC type I panel at failure

Figure 3.7 Typical view of BMC type II panel at failure

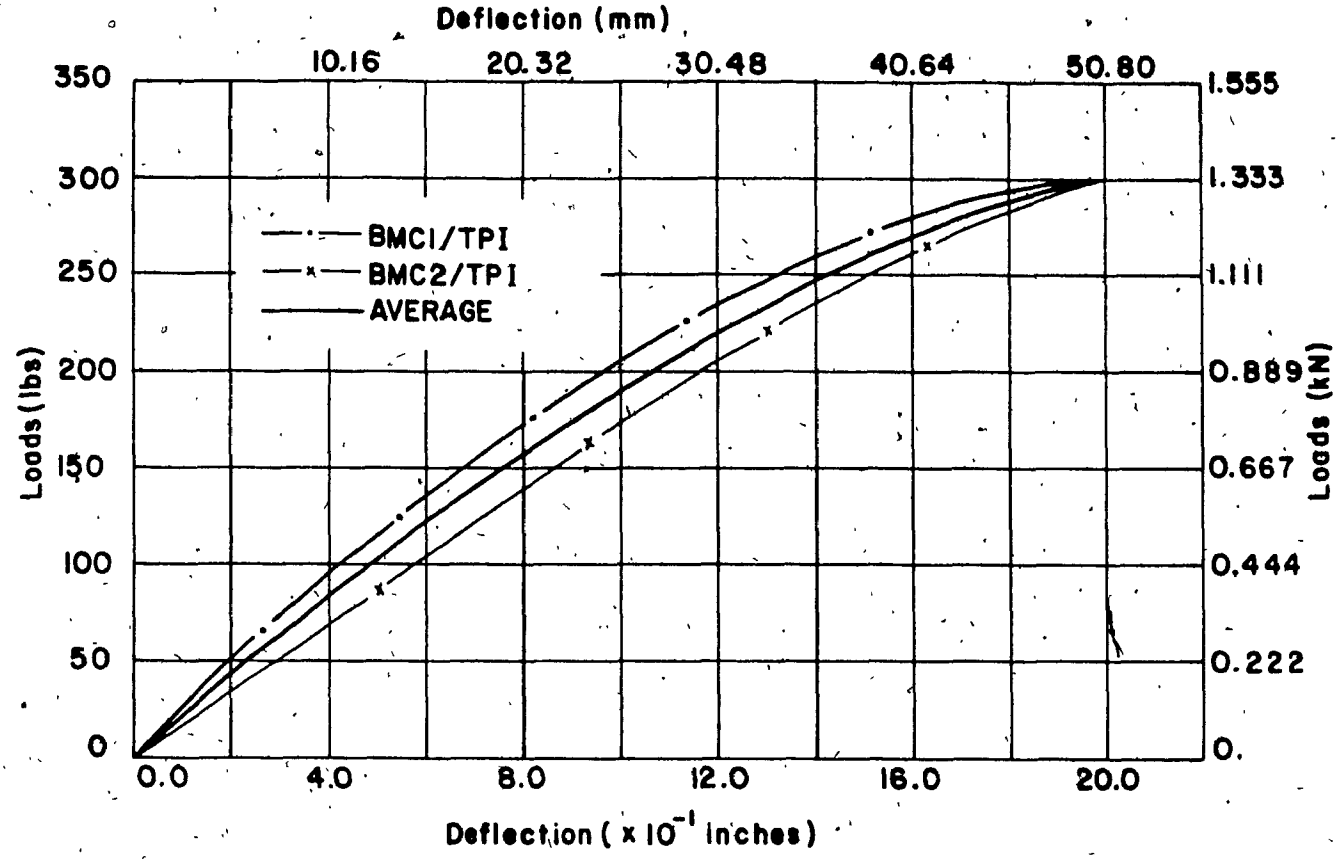

Figure 3.8 Load-deflection curves for BMC type I panels

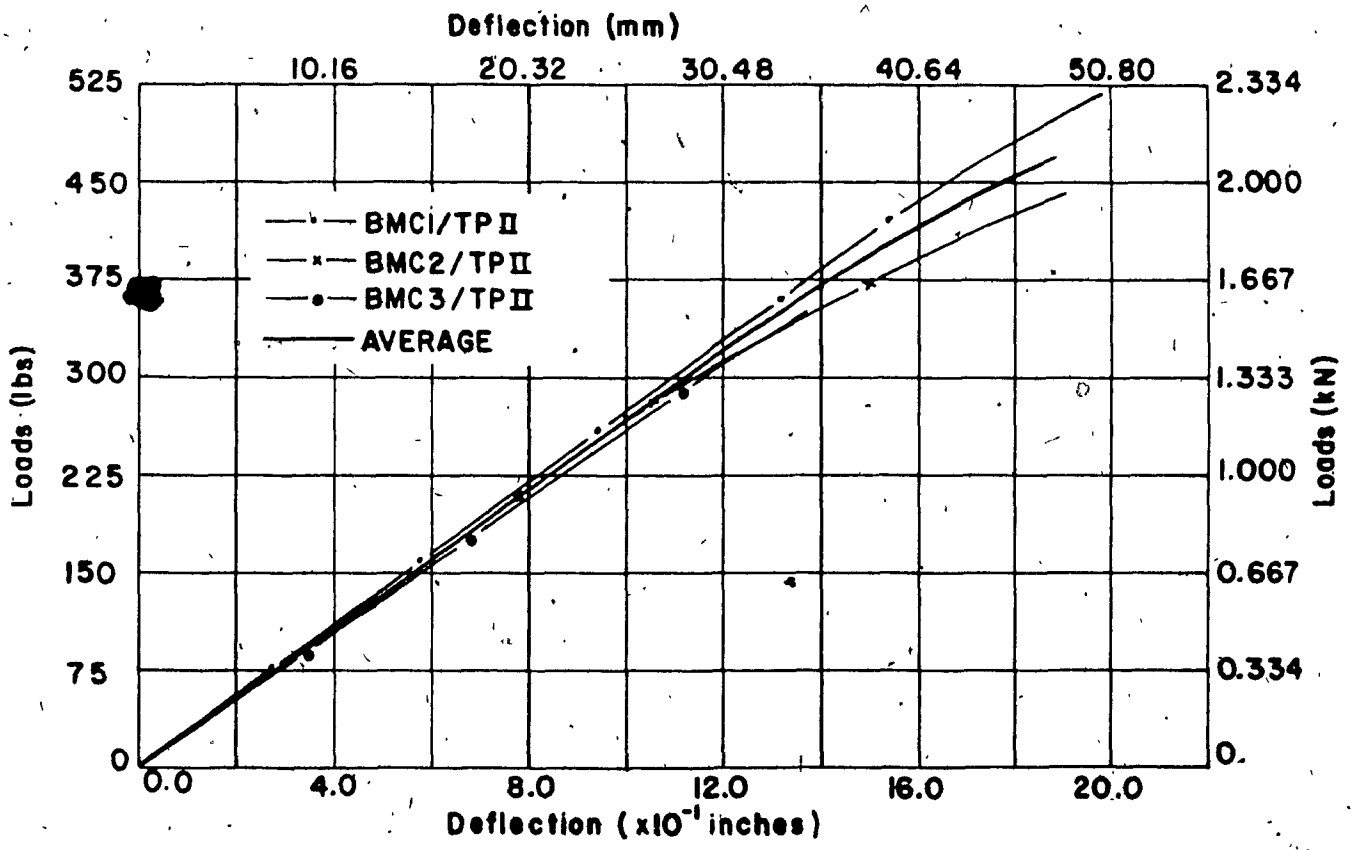

Figure 3.9 Load-deflection curves for BMC type II panels

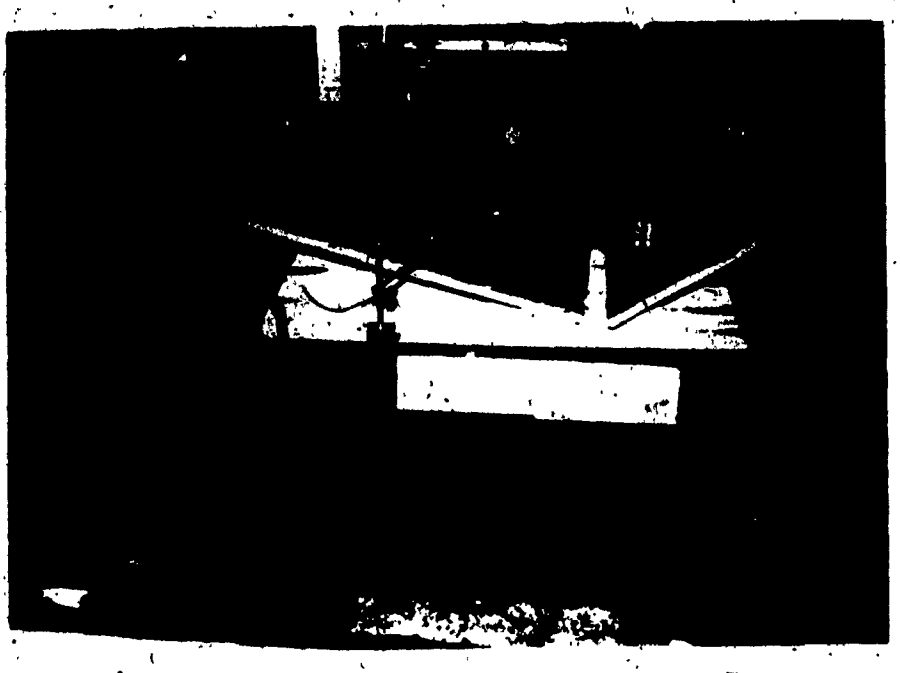

Figure 3.10 Typical view of BMCN type I panel at failure

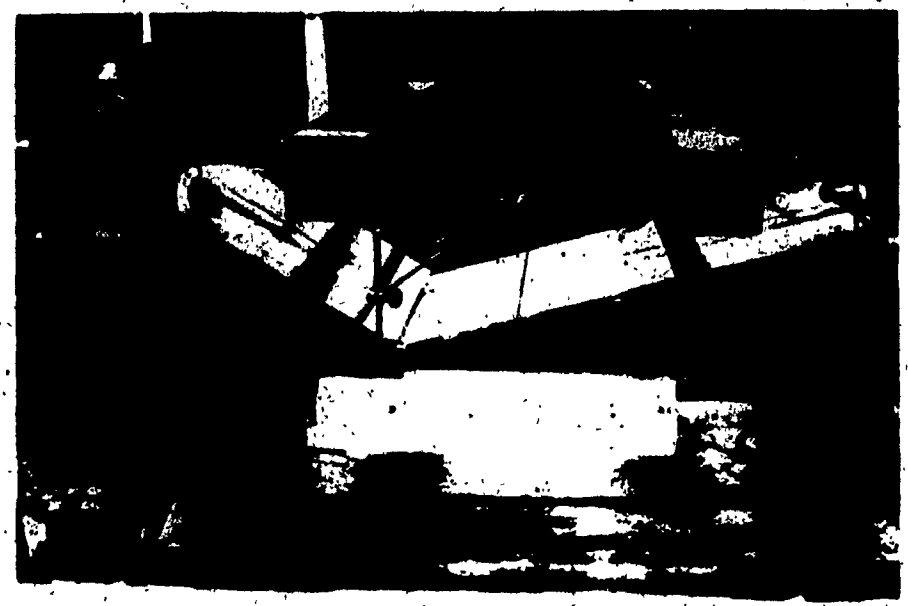

Figure 3.11 Typical view of BMCR type I panel at failure

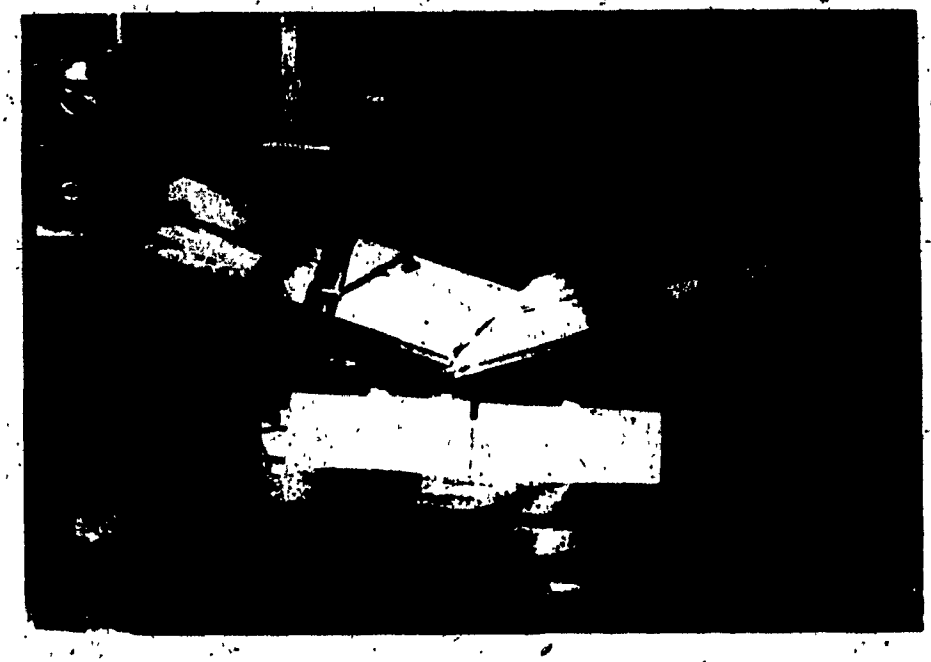

Figure 3.12 Typical view of BMCR type II panel at failure.

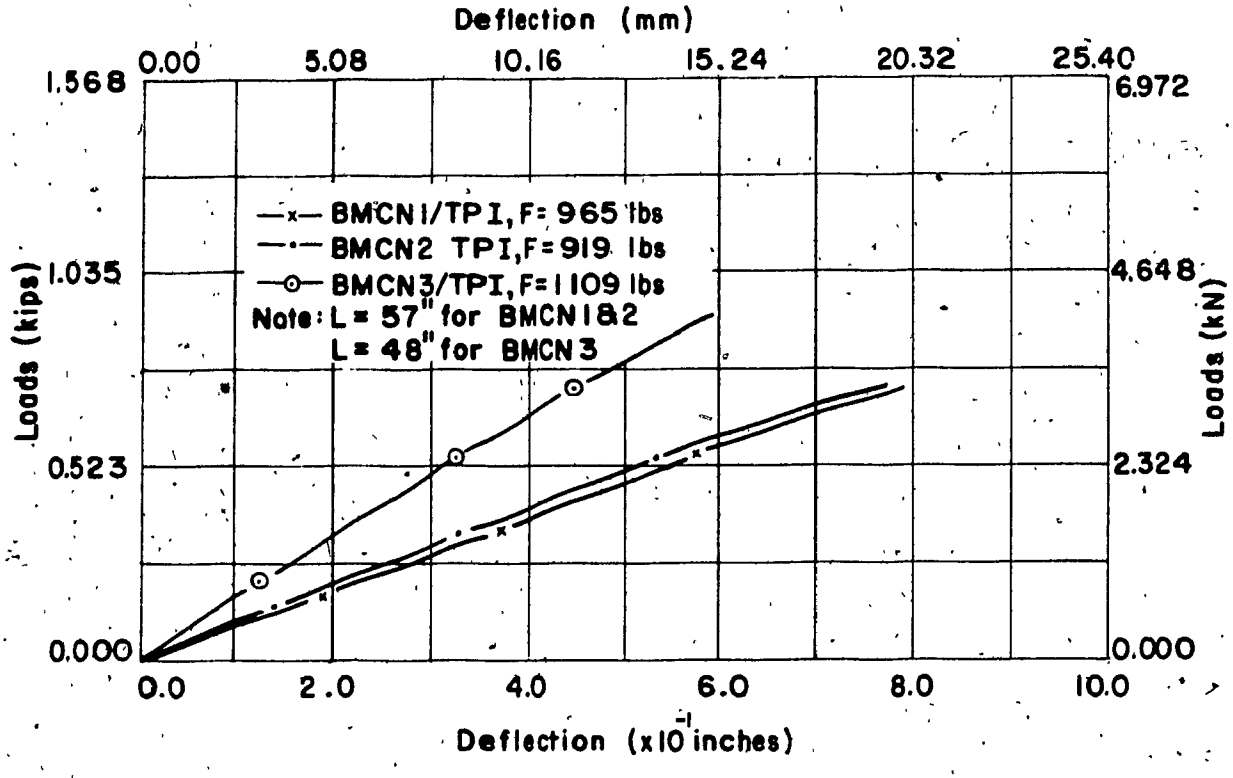

Figure 3.13 Load-deflection curves for BMCN type I panels

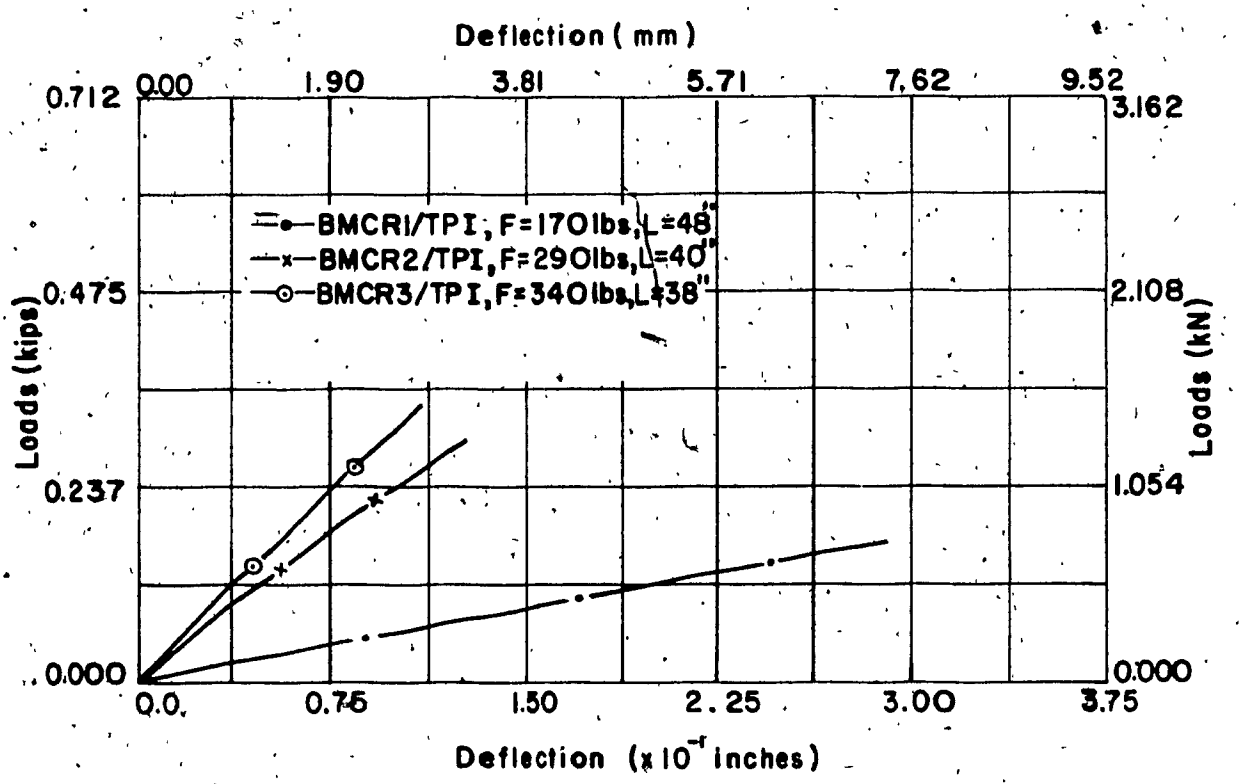

Figure 3.14 Load-deflection curves for BMCR type I panels

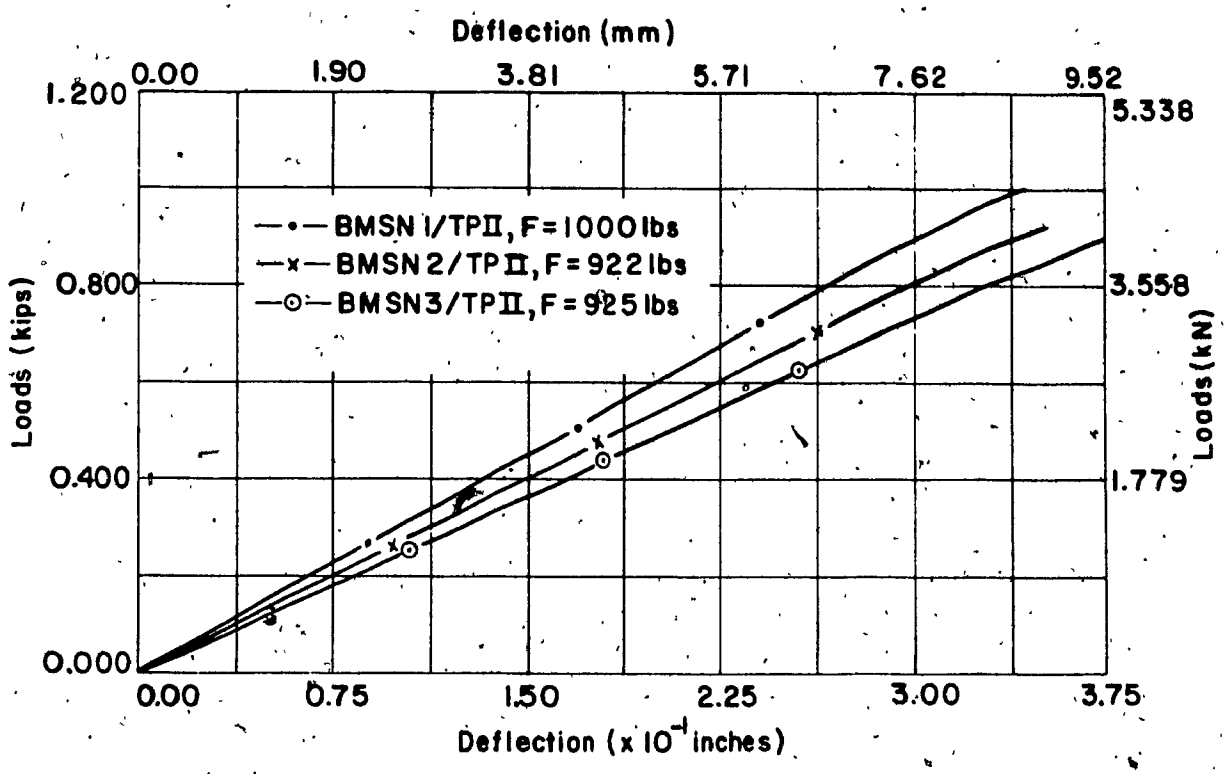

Figure 3.15 Load-deflection curves for BMSN type II panels

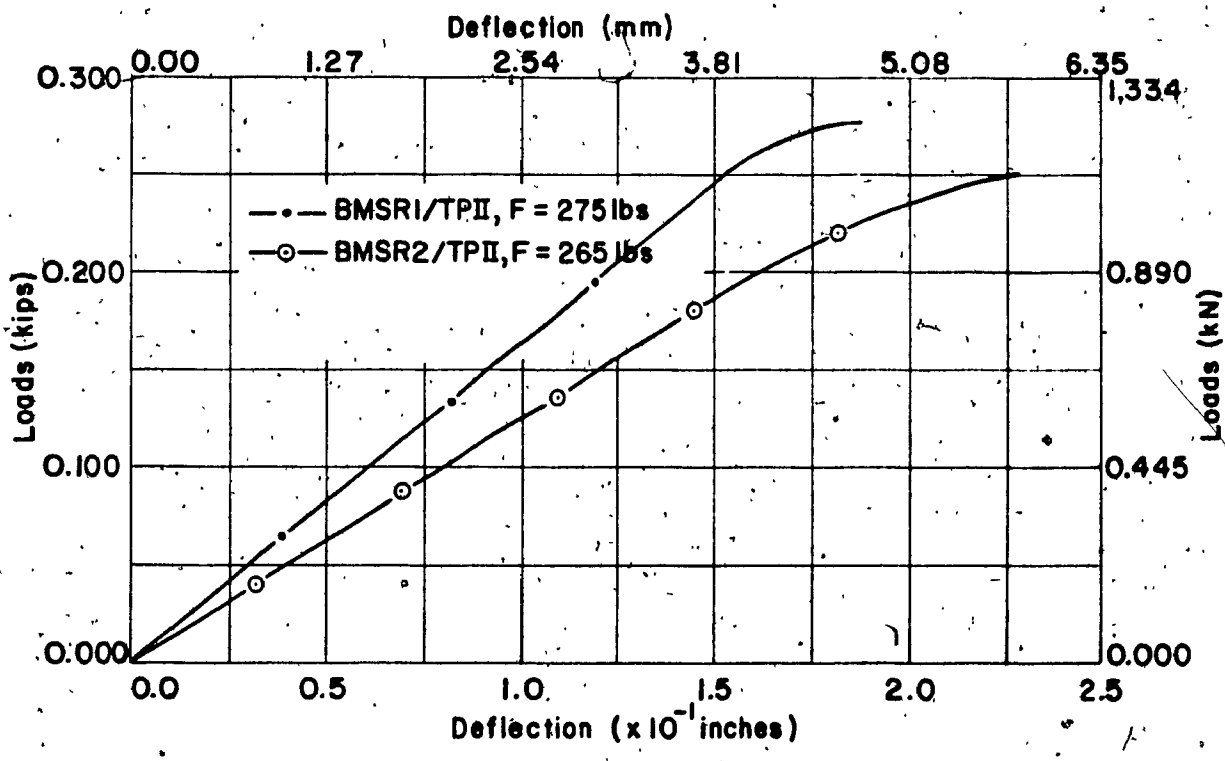

Figure 3.16 Load-deflection curves for BMSR type II panels

Figure 3.17 View of granite specimen (1-GP1) at failure

Figure 3.18 View of granite specimen (1-GP3) at failure

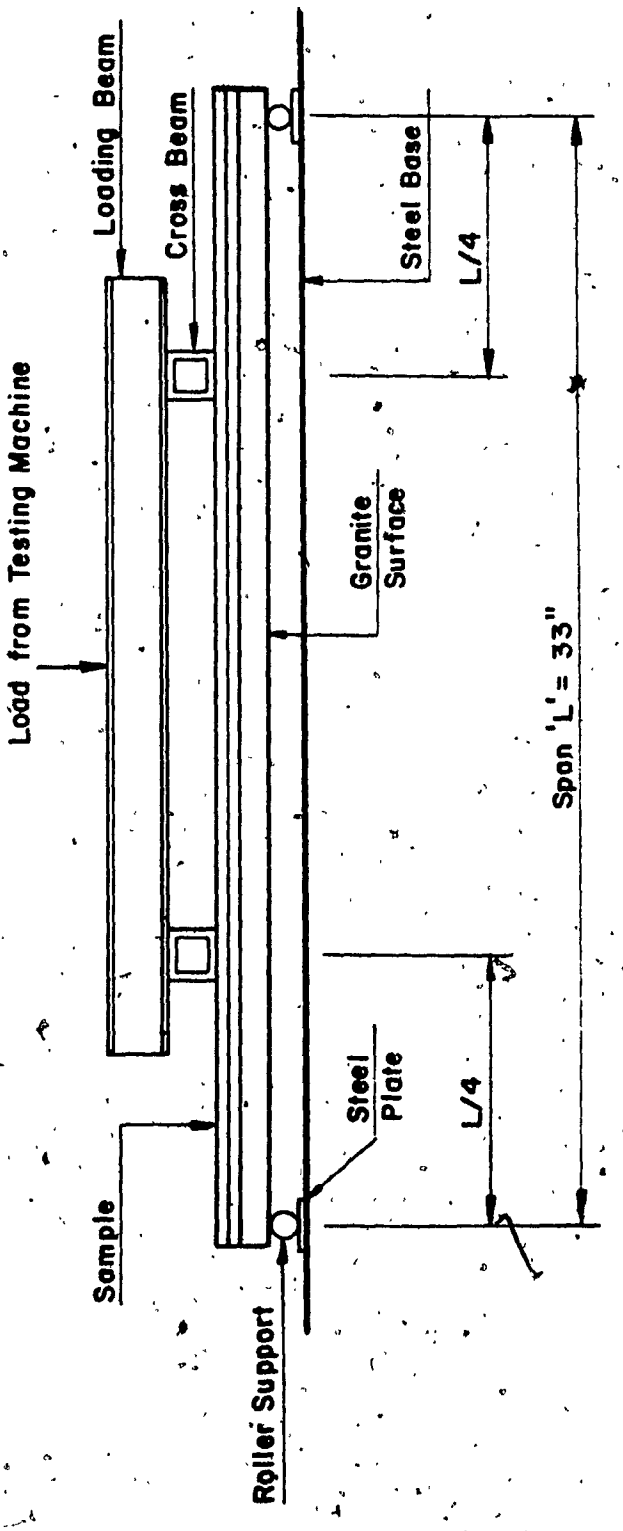

Figure 3.19 Testing arrangement for GFR panels

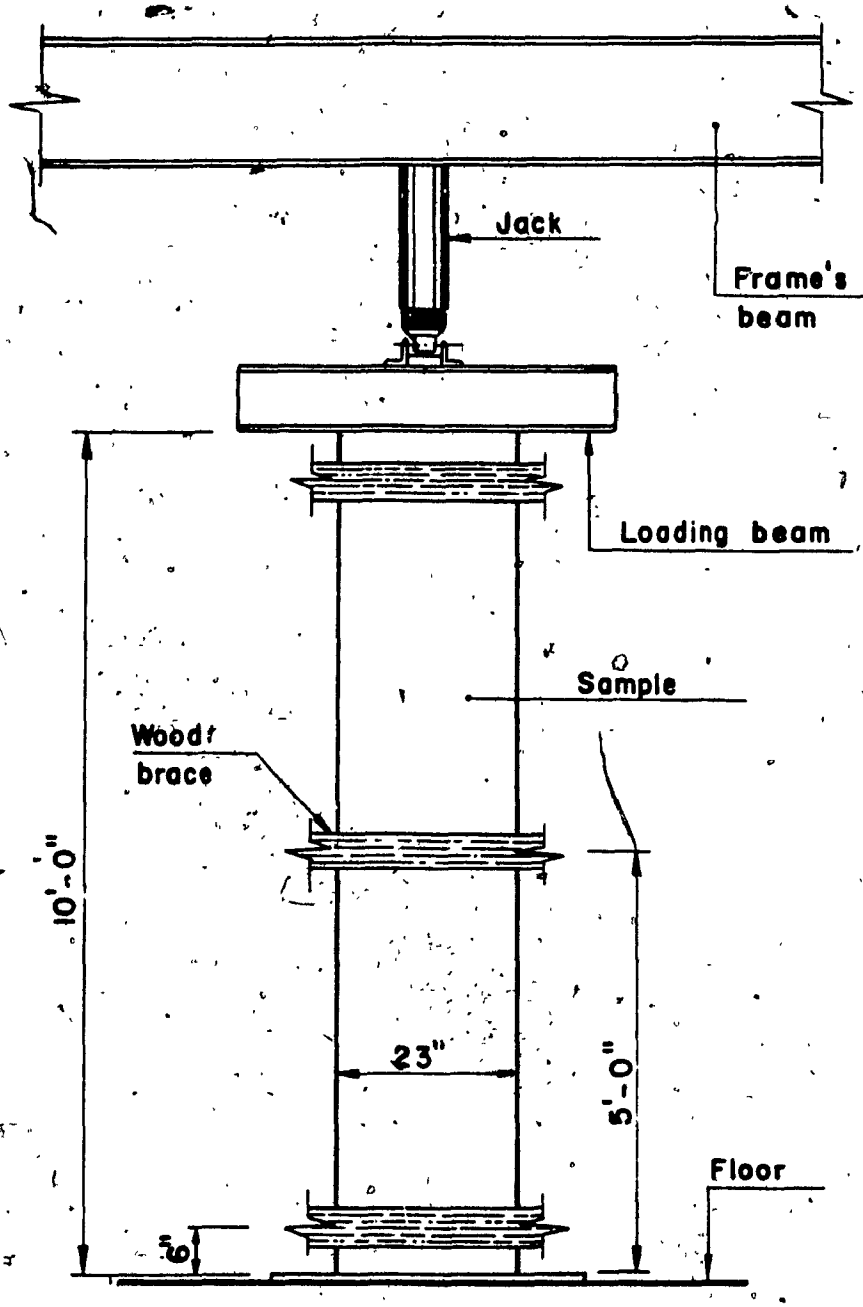

Figure 3.20 Experimental set-up for compression tests.

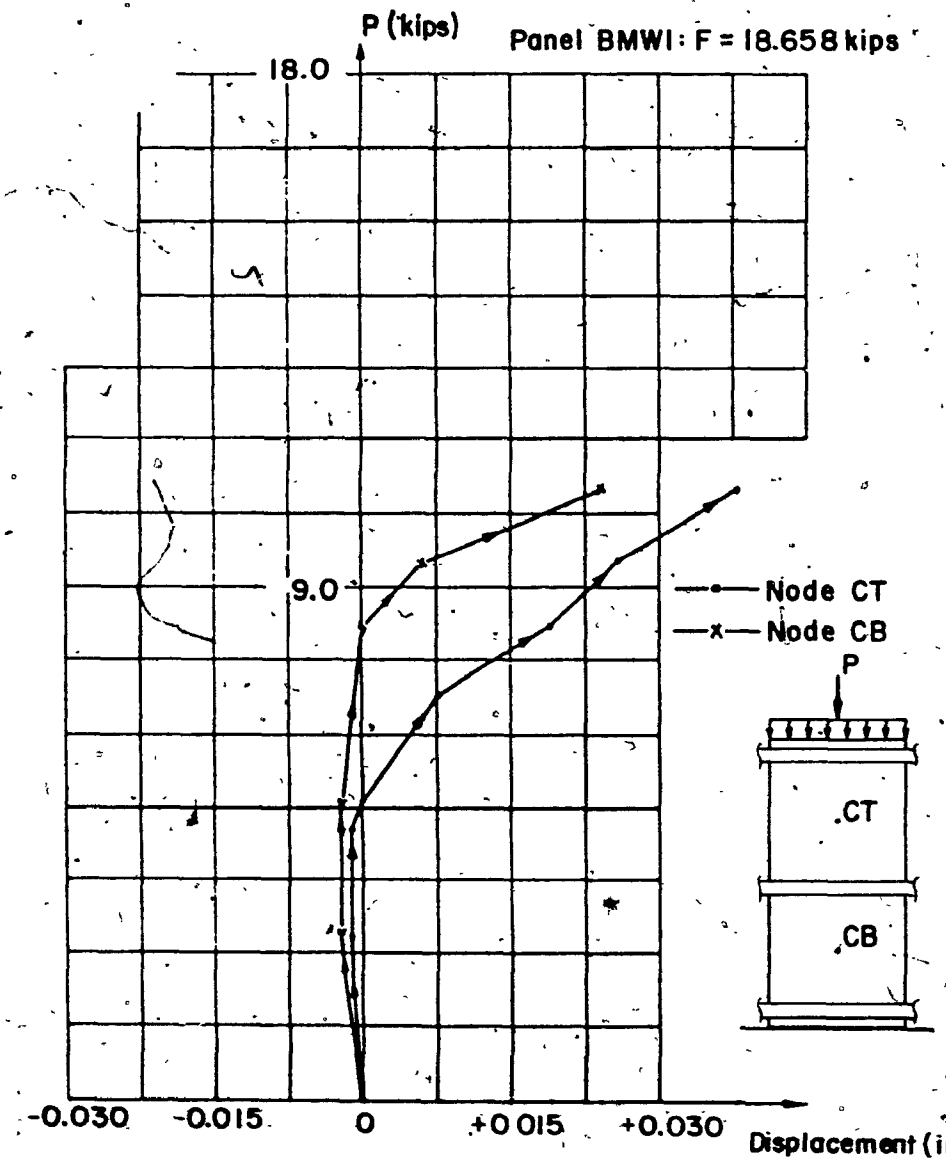

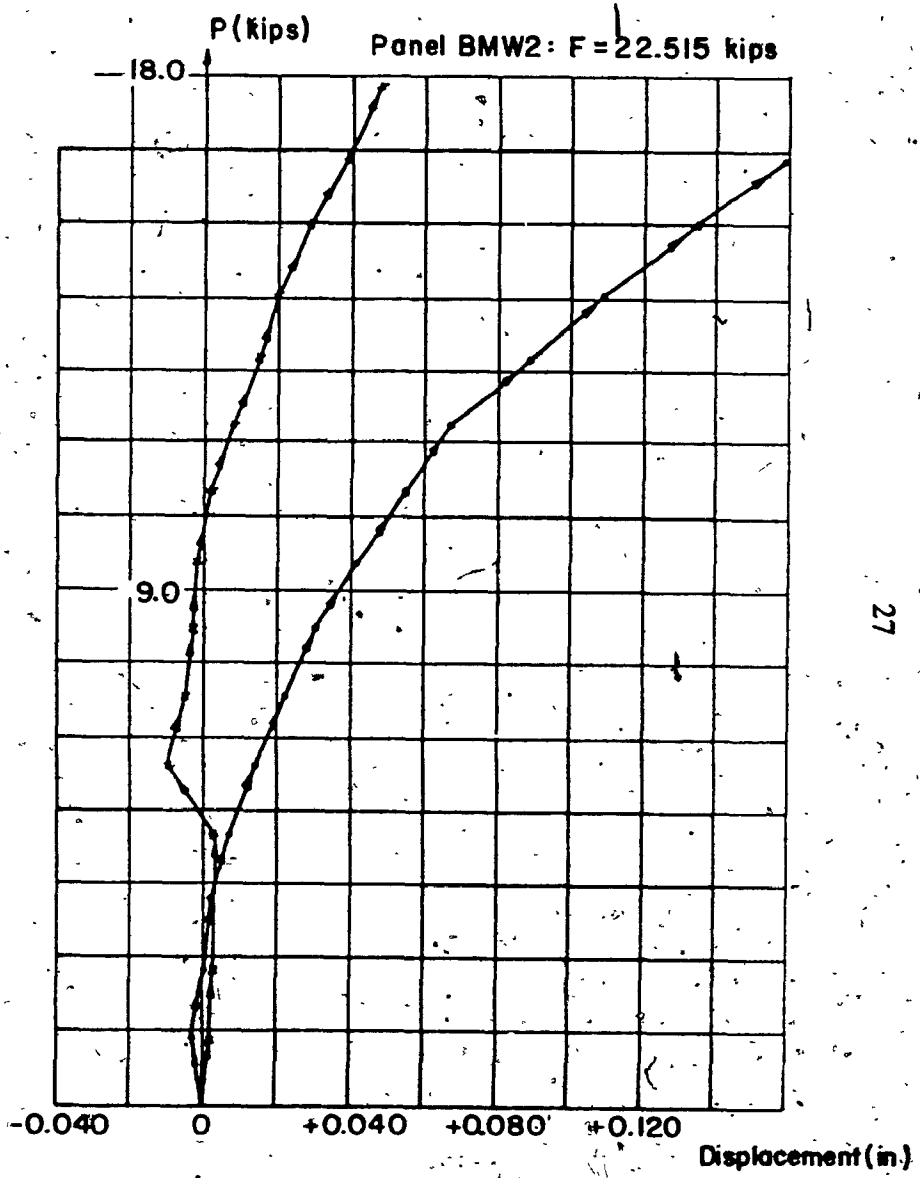

Figure 3.21 Horizontal displacements of nodes CT and CB

Figure 3.22 Mode of displacement of veneer specimen under compression prior to failure

Figure 3.24 Racking test arrangement for braced veneer specimen

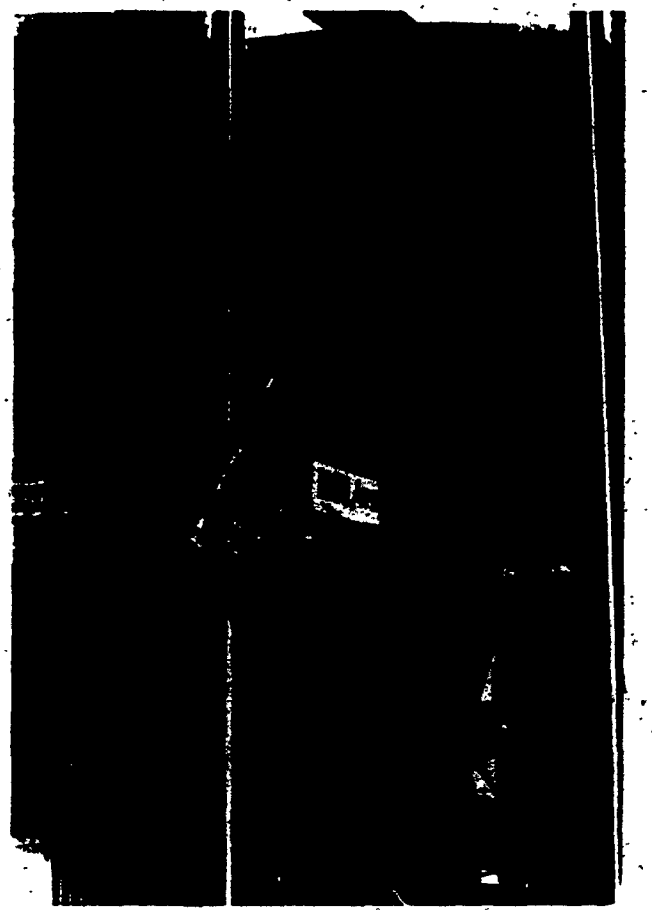

Figure 3.23 Racking test arrangement for unbraced veneer specimen

Figure 3.25 Typical view of unbraced veneer specimen under racking load (at failure)

Figure 3.26 Typical view of braced veneer specimen under racking load (at failure)

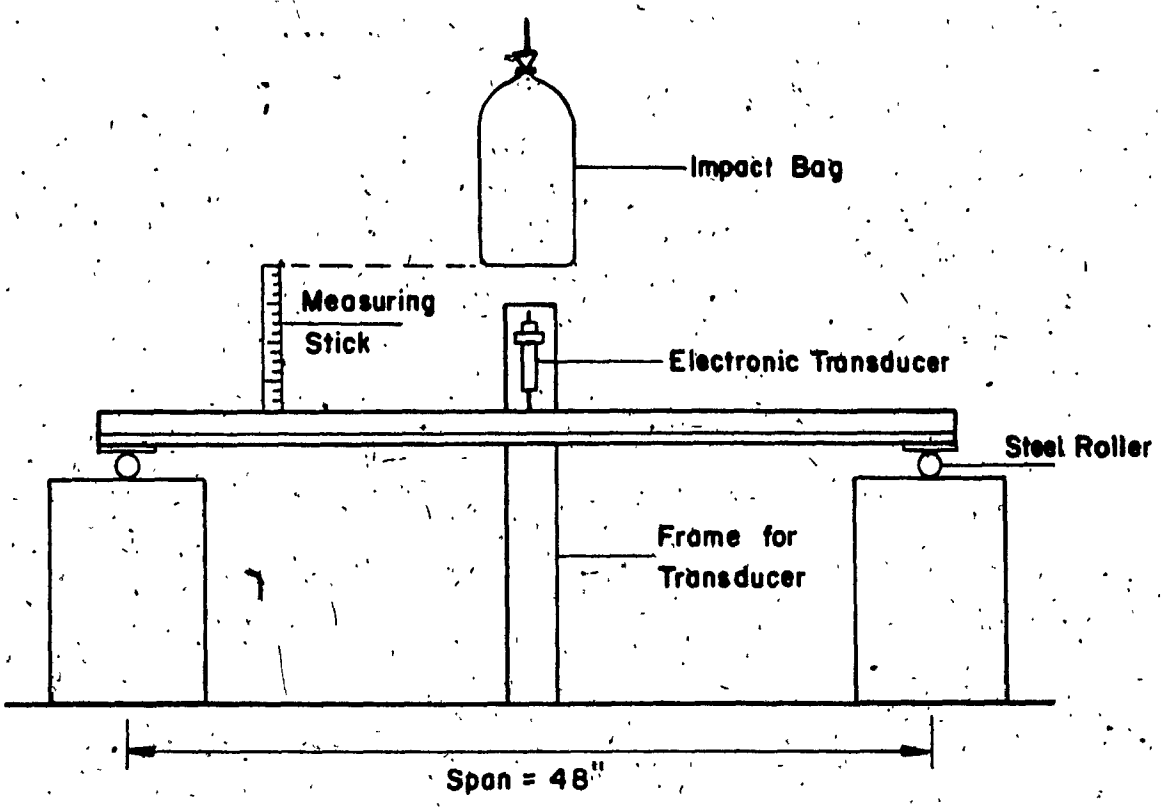

Figure 3.27 Testing arrangement for impact loading

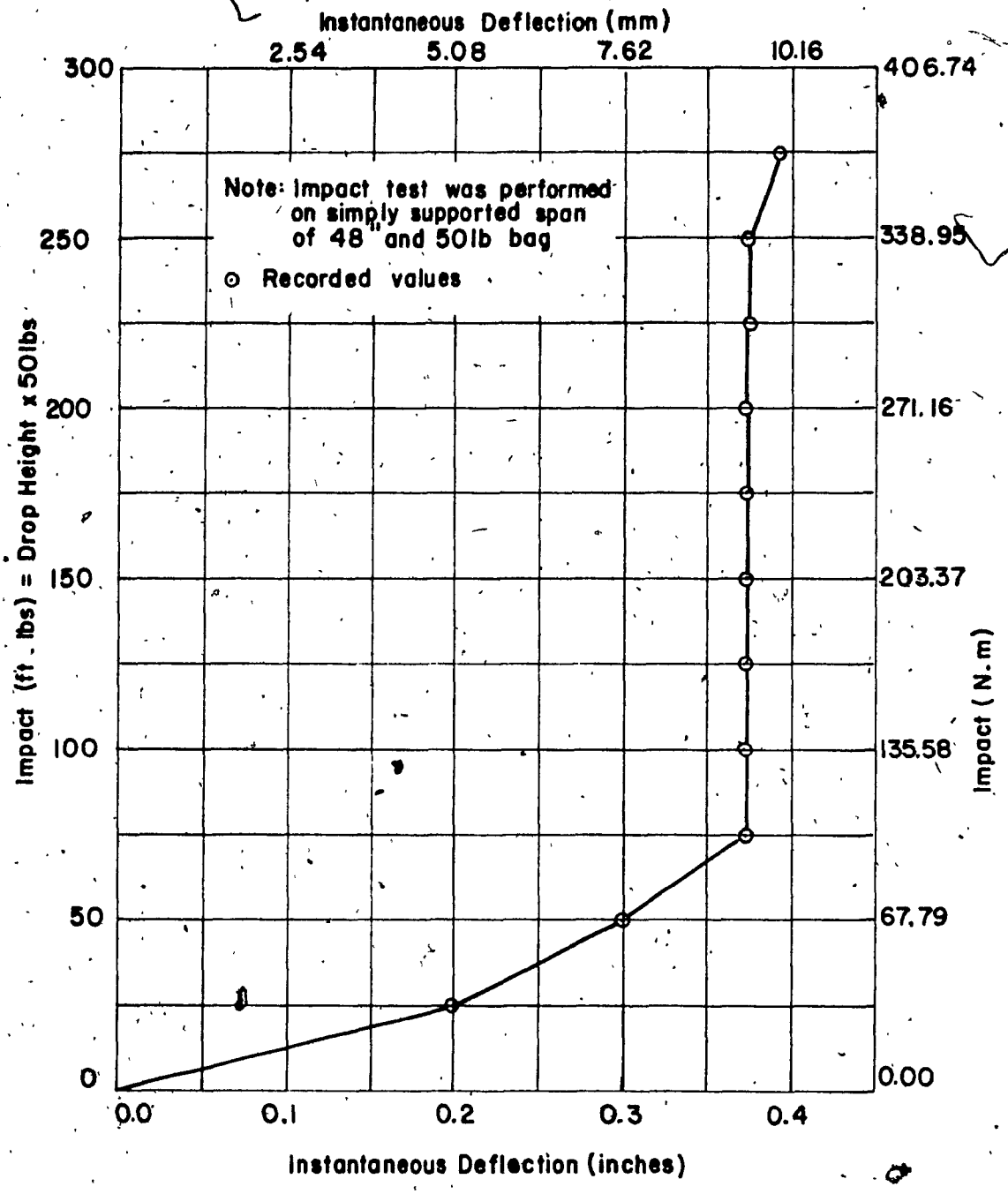

Figure 3.28 Drop-height vs. deflection curve for veneer specimen under

TEST SERIES	SAMPLE NO.	L (in)	W (in)	t_1 (in)	t_2 (in)	SCHEMATIC DIAGRAM
B1	BMC1/TP I	114	23	0.375	0.500	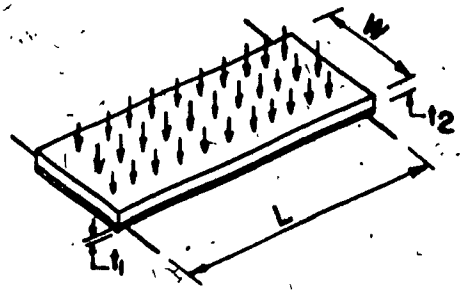
	BMC2/TP I	114	23	0.375	0.500	
	BMC1/TP II	114	23	0.375	0.500	
	BMC2/TP II	114	23	0.375	0.500	
	BMC3/TP II	114	23	0.375	0.500	
B2	BMCN1/TP I	57	23	0.375	0.500	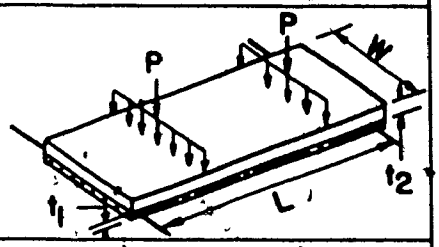
	BMCN2/TP I	57	23	0.375	0.500	
	BMCN3/TP I	48	23	0.375	0.500	
B3	BMCR1/TP I	48	23	0.375	0.500	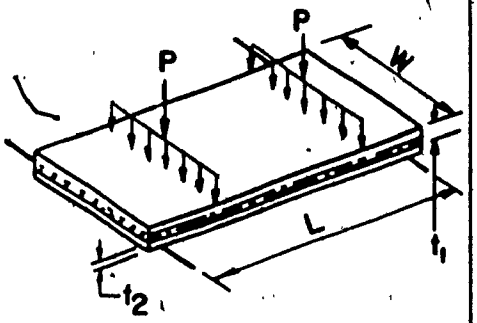
	BMCR2/TP I	40	23	0.375	0.500	
	BMCR3/TP I	38	23	0.375	0.500	
	BMCR1/TP II	48	23	0.375	0.500	
	BMCR2/TP II	48	23	0.375	0.500	
	BMCR3/TP II	48	23	0.375	0.500	
B4	BMSN1/TP II	48	23	0.375	0.500	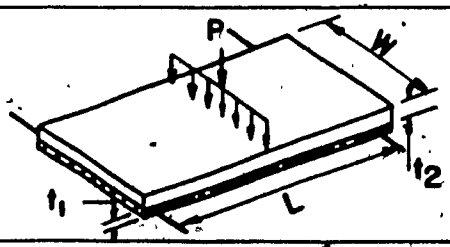
	BMSN2/TP II	48	23	0.375	0.500	
	BMSN3/TP II	48	23	0.375	0.500	
B5	BMSR1/TP II	48	23	0.375	0.500	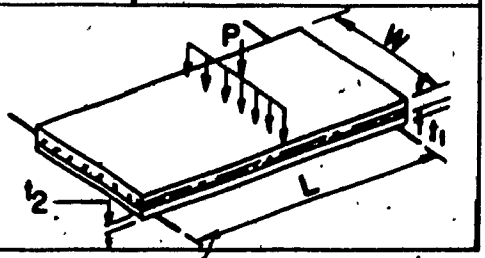
	BMSR2/TP II	48	23	0.375	0.500	
	BMSR3/TP II	48	23	0.375	0.500	

Table 3.1 Detailed descriptions of test series B1 - B5 for veneer specimens

TEST SERIES	SAMPLE NO.	L (in)	W (in)	t_1 (in)	t_2 (in)	t_3 (in)	SCHEMATIC DIAGRAM
G1	1-GP1	33	33	1.0	0.375	0.375	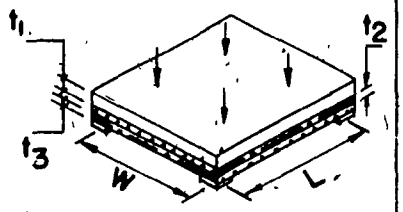
	1-GP2	33	33	1.0	0.375	0.375	
	1-GP3	33	33	1.0	0.375	0.375	
G2	2-GPR1	33	23.75	1.0	0.375	0.375	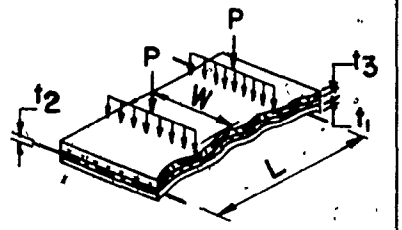
	2-GPR2	33	15.13	1.0	0.375	0.375	
	2-GPR3	33	13.44	1.0	0.375	0.375	

Table 3.2 Detailed descriptions of test series G1 for granite pavers

TEST SERIES	SAMPLE NO.	L (in)	W (in)	t_1 (in)	t_2 (in)	SCHEMATIC DIAGRAM
B6	BMW1/TPII	119.5	23	0.375	0.500	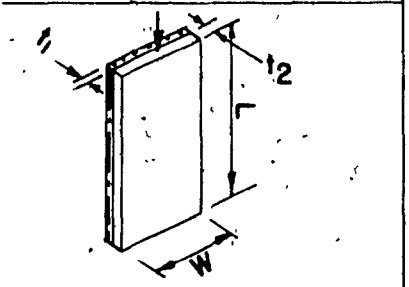
	BMW2/TPII	119.5	23	0.375	0.500	
B7	BMR1/TPII	60.0	48.0	0.375	0.500	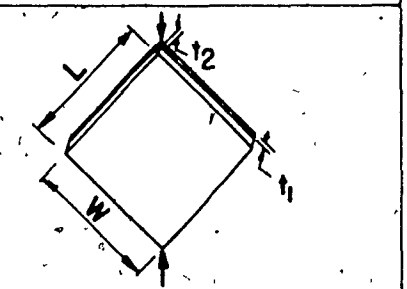
	BMR2/TPII	48.0	36.0	0.375	0.500	
B8	BMI/TPII	48.0	23.0	0.375	0.500	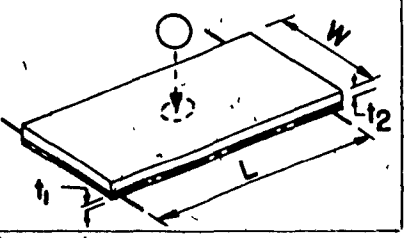

Table 3.3 Detailed descriptions of veneer panels used in compressive, racking and impact test

SAMPLE NO.	TOTAL FAILURE LOAD (kips)	EQUIVALENT ULTIMATE UNIFORM LOAD (lbs/sq.ft)	SCHEMATIC DIAGRAM
BMC1/TP I	0.482	26.5	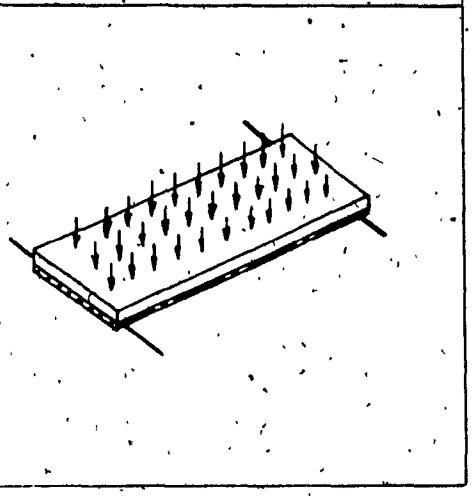
BMC2/TP I	0.502	27.6	
BMC1/TP II	0.632	34.7	
BMC2/TP II	0.572	31.4	
BMC3/TP II	0.702	38.6	

Table 3.4 Results for test series BMC

SAMPLE NO.	SPAN LENGTH (in)	TOTAL FAILURE LOAD (kips)	EQUIVALENT ULTIMATE UNIFORM LOAD (lbs/sq.ft)	SCHEMATIC DIAGRAM
BMCN1/TP I	57	1.056	115.99	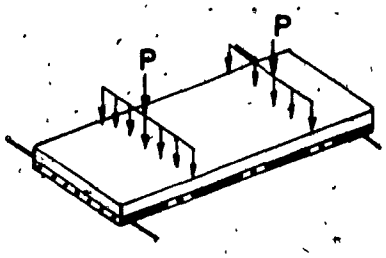
BMCN2/TP I	57	1.010	110.94	
BMCN3/TP I	48	1.186	154.70.	

Table 3.5 Results for test series BMCN

Sample No.	Span Length (in)	Total Failure Load '2P' (kips)	Equivalent Ultimate Uniform Load (lbs/sq.ft)	SCHEMATIC DIAGRAM
BMCR1/TPI	48	0.170	22.2	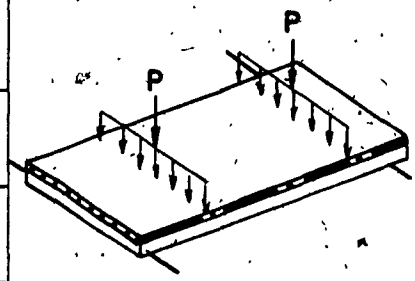
BMCR2/TPI	40	0.290	45.4	
BMCR3/TPI	38	0.340	56.0	
BMCR1/TPII	48	0.275	35.8	
BMCR2/TPII	48	0.289	37.7	
BMCR3/TPII	48	0.289	37.7	

Table 3.6 Results for test series BMCR

Sample No.	Span Length (in)	Total Failure Load 'P' (kips)	Equivalent Ultimate Uniform Load (lbs/sq.ft)	SCHEMATIC DIAGRAM
BMSN1/TPII	48	0.997	260.1	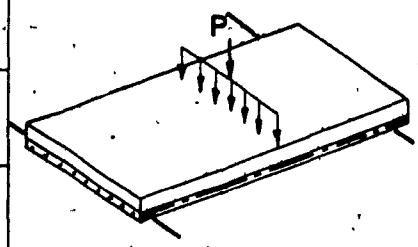
BMSN2/TPII	48	.922	240.5	
BMSN3/TPII	48	0.925	241.3	

Table 3.7 Results for test series BMSN

Sample No.	Span Length (in)	Total Failure Load 'P' (kips)	Equivalent Ultimate Uniform Load (lbs/sq.ft)	SCHEMATIC DIAGRAM
BMSR1/TPII	48	0.275	71.7	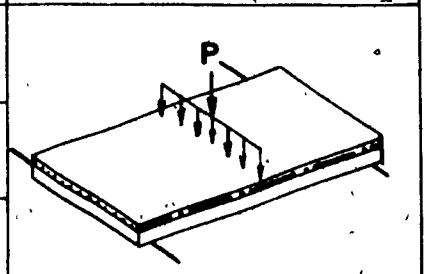
BMSR2/TPII	48	0.265	69.1	
BMSR3/TPII	48	0.270	70.4	

Table 3.8 Results for test series BMSR

Sample No.	Span Length (in)	Total Failure Load (kips)	Equivalent Ultimate Uniform Load lbs/sq.ft	SCHEMATIC DIAGRAM
I-GP1	33	17.931	2371	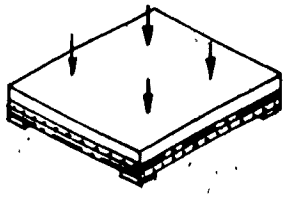
I-GP2	33	14.012	1853	
I-GP3	33	16.957	2242	

Table 3.9 Results for test series GP

Sample No.	Span Length (in)	Average Width (in)	Failure Load (kips)	Equivalent Ultimate Uniform Load (lbs/sq.ft)	SCHEMATIC DIAGRAM
2-GPR1	33	23.750	3.750	689	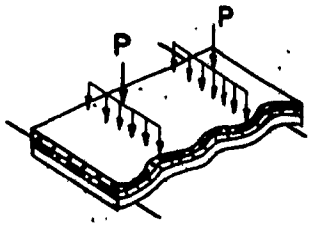
2-GPR2	33	15.125	2.627	652	
2-GPR3	33	13.437	2.027	658	

Table 3.10 Results for test series GPR

Sample No.	Critical Height (in)	Failure Load (kips)	SCHEMATIC DIAGRAM
BMW1/TPII	52	18.658	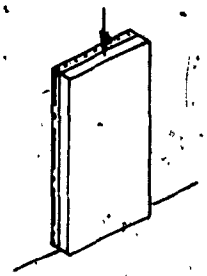
BMW2/TPII	52	22.515	

Table 3.11 Results for compressive bearing capacity veneer panels

CHAPTER IV

STRENGTH EVALUATION AND PROPOSED DESIGN PROCEDURE FOR COMPOSITE FIBRE REINFORCED PANELS

4.1 Cracking Strength of Asbestos - Cement Members Loaded in Bending

Practice introduced by De Mahieu [4] for calculating the flexural strength of asbestos - cement beams is based on an assumption that the concentrated compressive force acts at the top of the beam cross section while the tensile stress follows a triangular distribution as shown in Figure 4.1. The section falls when the maximum tensile strength is reached at the bottom fibre.

Calculations based on the above theory gives, for rectangular sections, results comparable with tests, but rather deviating results for non symmetric sections. This theory does not confirm the true behavior of fibre reinforced cement materials such as asbestos - cement, which under high tensile stress close to failure, demonstrates an elasto-plastic mode of behavior [12, 13].

Based on research work on flexural strength of ferrocement [15, 16, 17] and reinforced and plain concrete [5, 6, 18], it appears justified to expect that flexural strength of asbestos - cement can be best predicted assuming a stress distribution shown in Figure 4.2 and in simplified form for design practice as shown in Figure 4.3 (c). Based on tests, it can also be assumed that the maximum strain at failure, close to the bottom tension zone, is equal to:

$$\varepsilon_{ct} = 0.001.$$

Corresponding to this strain, the stress in reinforcing steel, if present, will be:

$$f_s = \varepsilon_{ct} \cdot E_s = 29.0 \text{ ksi } (200.0 \text{ Mpa}).$$

Figure 4.3 shows a generalized I - shaped section at failure (cracking), a strain diagram and a simplified stress diagram. The I-shaped section is obtained by transforming the non-symmetric section into an equivalent rectangular section, with the flanges and reinforcement representing the required additional areas .

The following relationships can be noted, based on Figure 4.3 (c):

$$f_{cc} = 2f_{to}\left(\frac{x}{x-h}\right) \qquad (4.1)$$

$$f'_s = 2nf_{to}\left(\frac{x-d''}{h-x}\right) \qquad (4.2)$$

In the above equations, n denotes the modular ratio (E_s/E_c) and f_{to} is the flexural tensile strength of asbestos - cement. From the equilibrium of forces $\Sigma P = 0$,

$$nA'_s f'_s + \Delta A'_c f_{ci} + 1/2(bxf_{cc}) - b(h-x)f_{to} - \Delta A_c f_{to} - A_s f_s = 0 \qquad (4.3)$$

After substituting values from (4.1) and (4.2) into equation (4.3), x is obtained as follows:

$$x = \frac{1 + \left[\frac{\Delta A_c f_{to} + A_s f_s}{bhf_{to}}\right]}{2 + 2\left[\frac{\Delta A'_c + nA'_s}{bh}\right] + \left[\frac{\Delta A_c f_{to} + A_s f_s}{bhf_{to}}\right]}(h) \qquad (4.4)$$

Equation (4.4) can be rewritten as:

$$\frac{x}{h} = \frac{1 + \psi_t}{2 + 2\psi_c + \psi_t} \qquad (4.5)$$

where ψ_t and ψ_c are the shape factors describing the strengthening in the tension and compression zone respectively of basic rectangular section.

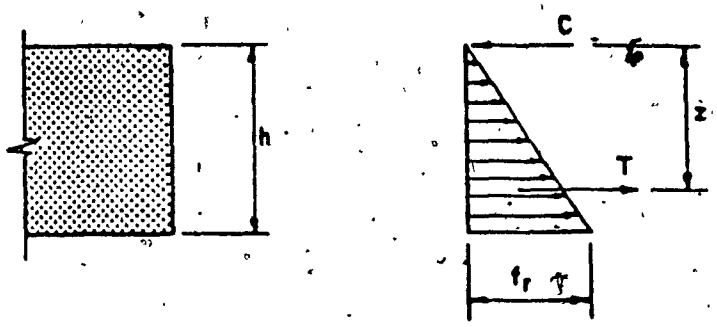

Figure 4.1 Stress distribution at failure based on De-Mahieu hypothesis: (a) section; (b) stresses

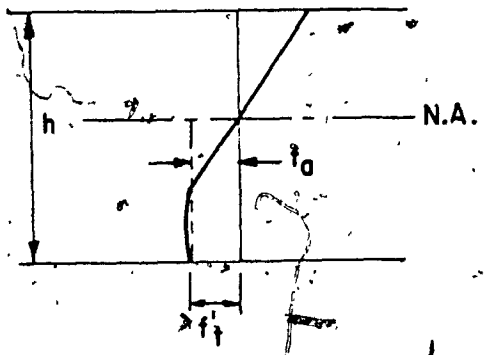

Figure 4.2 Stresses in concrete beam immediately before cracking

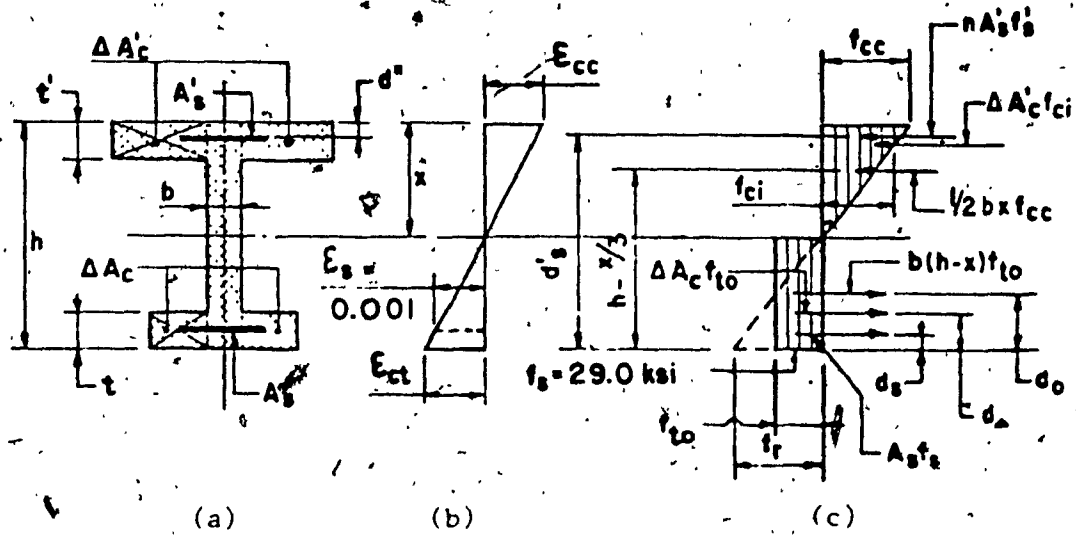

Figure 4.3 Generalized I-shaped section at cracking: (a) cross-section; (b) strain diagram; (c) simplified stress diagram

$$\psi_t = \frac{\Delta A_c f_{to} + A_s f_s}{bhf_{to}}$$

$$\psi_c = \frac{\Delta A'_c + nA'_s}{bh} \qquad (4.6)$$

If there are no flanges (rectangular section) ΔA_c and $\Delta A'_c$ are equal to zero and:

$$\psi_t = \frac{A_s f_s}{bhf_{to}} \; ; \; \psi_c = \frac{nA'_s}{bh}$$

If there is no tension reinforcement A_s, then $\psi_t = 0$, and if there is no compression reinforcement A's, then $\psi_c = 0$.

The flexural cracking strength can be now calculated from the equilibrium of moments, $\Sigma M = 0$, as follows:

$$M_{cr} = f_{to} bh^2 (A + B\psi_t + \Sigma \psi_{ti} \delta_i) \qquad (4.7)$$

where,

$$A = \frac{1}{2} - \frac{\gamma\psi_c}{1 + 2\psi_c} - \frac{1 - 2\psi_c}{6(1 + 2\psi_c)} - \frac{1}{6}\left[\frac{1 + 2\psi_c}{2 + 2\psi_c}\right]^2$$

$$B = 1 - \frac{\gamma\psi_c}{1 - 2\psi_c} - \frac{1}{3(1 + 2\psi_c)} \qquad (4.8)$$

$$\gamma = \frac{t'}{h}$$

$$\Sigma \psi_{ti} \delta_i = \frac{\Delta A_c d_\Delta}{bh^2} + \frac{A_s f_s d_s}{bh^2 f_{to}}$$

Table 4.1 gives the values of A and B for different ψ_t, ψ_c and γ values.

From the equations shown, it is possible to calculate the flexural cracking moment of any geometrical section. The procedure of calculation consists of the following steps:

(a) transform the actual cross-section into an equivalent rectangular section;

(b) find all the necessary coefficients (ψ_t, ψ_c, A, B, γ and $\Sigma\psi_{ti}\delta_i$);

(c) consider a value of f_{to} based on recorded test results or obtained from the rupture strength (by using a shape factor ψ) which varies from 1.75 for rectangular to 1.25 for I - sections [10, 11]; and

(d) apply equation (4.7) to find the cracking moment M_{cr}

These steps have been used successfully in predicting the flexural cracking strength of asbestos - cement panels made of 'v' and 'u' shaped sections tested at Concordia structural laboratories earlier [7, 8].

The present research work is carried out to verify the applicability of equation (4.7) for thin composite sections made of natural stone and one or two layers of asbestos - cement densite sheets.

4.1.1. Flexural Cracking Strength of Veneer Panels

At low loads, 'veneer' panels, as tested, demonstrated an elastic behavior (Figure 4.4) and the neutral axis is located in the asbestos - cement part of the cross-section. With increasing loads, the asbestos - cement part of the panel (under tension) reaches the plastic stage. The neutral axis rises and part of the marble is now under tension. This behavior compares with results obtained by Allen [9] for thin flexural specimens of composites. Failure occurs when the ultimate tensile strain of asbestos - cement is reached at the bottom. Based on this observation, the following assumptions can be made for the flexural strength analysis:

(1) the stresses in the tensile zone can be represented by a constant stress f_{tm} across the tension zone (Figures 4.5 (c) and (d)); and

(2) the tensile contribution of asbestos - cement layer (densite) is represented by a force $T_{asb} = (f_{tol} - f_{tm})A_{asb}$, and where $(f_{tol} - f_{tm})$ is the difference between the tensile strength of asbestos - cement and marble.

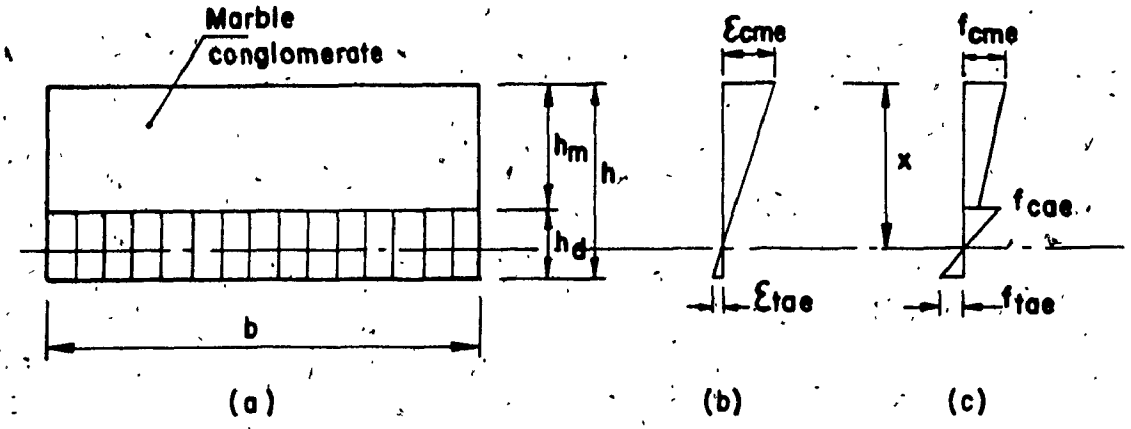

Figure 4.4. The State of Strain and Stress for Veneer Section at Elastic Stage: (a) cross - section, (b) strain diagram, (c) stress diagram.

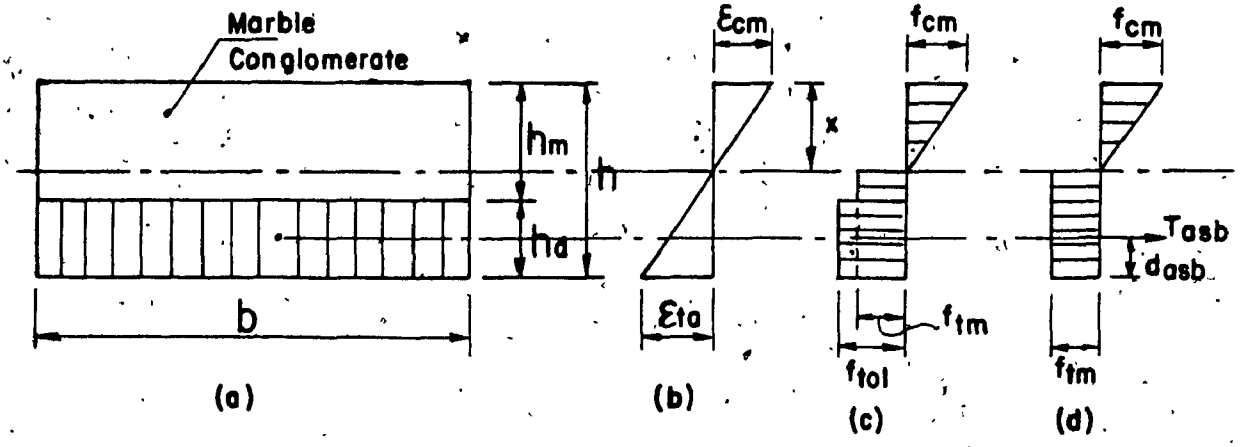

Figure 4.5. Assumptions for the Analysis Method (veneer section): (a) cross - section; (b) strain diagram; (c) assumed stress distribution; (d) simplified representation.

The location of the neutral axis of the cross - section at cracking can be defined using equation (4.4) or (4.5) which in this case may be written as follows:

$$\frac{x}{h} = \frac{1 + \frac{h_d}{h}\left[\frac{f_{tol} - f_{tm}}{f_{tm}}\right]}{2 + \frac{h_d}{h}\left[\frac{f_{tol} - f_{tm}}{f_{tm}}\right]} \qquad (4.9)$$

In this case, the coefficients of strengthening of section in tension and compression are given as follows:

$$\psi_t = \frac{h_d}{h}\left[\frac{f_{tol} - f_{tm}}{f_{tm}}\right] \qquad (4.10)$$

$$\psi_c = 0$$

The coefficients A, B and γ for calculating the flexural cracking moment of the veneer panel can then be established as follows:

$$A = 0.292 \quad ; \quad B = 0.667 \quad ; \quad \gamma = 0$$

Further, it can be calculated

$$\Sigma \psi_{ti}\, \delta_i = \frac{h_d}{h}\left[\frac{f_{tol} - f_{tm}}{f_{tm}}\right]\frac{d_{asb}}{h} \qquad (4.11)$$

The flexural cracking moment, based on equation 4.7, can then be expressed as:

$$M_{cr} = f_{tm}\, bh^2 \left[0.292 + \frac{0.667 h_d}{h}\left[\frac{f_{tol} - f_{tm}}{f_{tm}}\right] - \frac{h_d d_{asb}}{h^2}\left[\frac{f_{tol} - f_{tm}}{f_{tm}}\right]\right] \qquad (4.12)$$

Comparison of calculated and test recorded capacities are shown in Table 4.2. As seen from this Table, the computed values are very close to the tested values. Therefore, the foregoing method of analysis can be recommended for design practice. Detailed calculations of composite veneer panels tested are shown in Appendix A.

4.1.2 Flexural Cracking Strength of Granite Paver

The presence of two layers of asbestos - cement sheet with their fiber directions oriented perpendicular to each other modifies the stress distribution assumed in section 4.1.1. Noting that at failure, the bottom layer breaks along the longitudinal fiber direction (loaded perpendicular to its fibers) and which has a lower strength than the upper asbestos - cement layer (loaded in the direction of the fibers). The neutral axis lies in the vicinity of the granite-densite interface, the following assumptions can be made for the analysis methods:

(a) the stresses in the tensile zone can be represented by a constant stress f_{tot} across the bottom layer and a constant stress f_{tol} across the upper layer (Figure 4.6 (c)); and

(b) the tensile contribution of the upper asbestos - cement layer can be represented by a force:

$$T'_{asb} = (f_{tol} - f_{tot})A_{asb}$$

where $(f_{tol} - f_{tot})$ is the difference between the flexural tensile strength of asbestos - cement (densite) loaded in the longitudinal and transverse directions (Figure 4.6 (d)).

The location of the neutral axis at the cracking stage in this case is given as follows:

$$\frac{x}{h} = \frac{1 + \frac{h_{d1}}{h}\left[\frac{f_{tol} - f_{tot}}{f_{tot}}\right]}{2 + \frac{h_{d1}}{h}\left[\frac{f_{tol} - f_{tot}}{f_{tot}}\right]} \qquad (4.13)$$

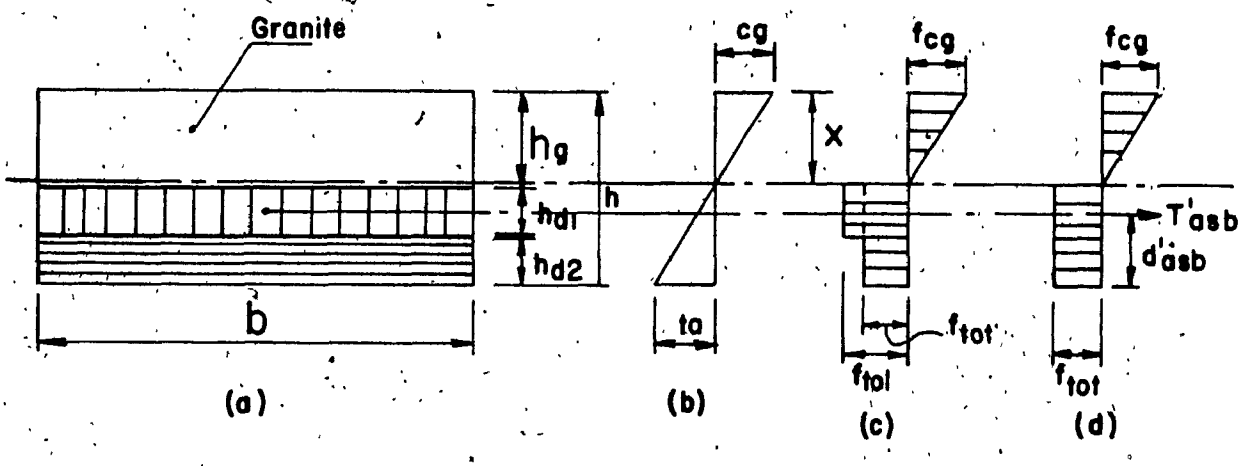

Figure 4.6. Assumptions for the Analysis Method (granite pavers):
(a) cross - section; (b) strain diagram; (c) assumed stress distribution;
(d) simplified representation.

The coefficients for the strengthening of a section in tension and compression are given as:

$$\psi_t = \frac{h_{d1}}{h}\left[\frac{f_{tol} - f_{tot}}{f_{tot}}\right] \qquad (4.14)$$

$$\psi_c = 0$$

The coefficients for calculating the flexural cracking moment of granite pavers can be established as follows:

$$A = 0.292 \quad ; B = 0.667 \; ; \quad \gamma = 0$$

$$\Sigma \psi_{ti} \delta_i = \frac{h_{d_1} d_{asb}}{h^2} \left[\frac{f_{tol} - f_{tot}}{f_{tot}} \right] \tag{4.15}$$

and the flexural cracking moment can then be expressed as:

$$M_{cr} = f_{tot} bh^2 \left[0.292 + \frac{0.667 h_{d_1}}{h} \left[\frac{f_{tol} - f_{tot}}{f_{tot}} \right] - \frac{h_{d_1} d_{asb}}{h^2} \left[\frac{f_{tol} - f_{tot}}{f_{tot}} \right] \right] \tag{4.16}$$

Calculated results and tested results are compared in Table 4.3. Detailed calculations are given in Appendix B.

4.2 Determination of Safe Service Load (in Flexure)

Service loads are defined normally based on prescribed load factors. Building codes normally prescribe different load factors for dead and live loads together with various load combinations. For reinforced concrete structures, the 1983 ACI Code [10] recommends overload factors of 1.4 and 1.7 for dead load and live load respectively. The products of lamination of asbestos - cement and natural stones normally have thin thickness, and hence, the dead weight is insignificant as compared to the imposed live load. Therefore, single value of load factor of $S_1 = 1.7$ can be used for all loads (dead and live). However, introduction of an additional capacity reduction factor is required to reflect the degree of ductility of the member under the load effects being considered.

While asbestos - cement elements collapse under flexure in a semi-brittle manner at the moment of cracking, reinforced concrete members will not collapse when concrete cracks in the tension zone and even later when the tension steel yields. Normally,

reinforced concrete structures collapse after the rupture strength of steel has been reached, which is 70% higher than the yield strength as used in the ultimate strength design. In order to put the composite products of asbestos - cement and natural stones at par with reinforced concrete in terms of safe and failure loads, it is proposed to consider an additional load factor of $S_2 = 1.35$. The overall proposed factor of safety becomes:

$$S = S_1 \times S_2 = 1.7 \times 1.35 = 2.295 \approx 2.3.$$

or more conservatively, a factor of safety of $S = 2.5$ should be used for structures erected on site where adequate technical supervision is not warranted.

Consequently, the following design procedure can be adopted for composite products of asbestos - cement and natural stones:

1. establish the service loads based on the intended use of the products;
2. multiply the service loads by a factor of 2.3 for products produced in a controlled type condition or by a factor of 2.5 for products erected on site where adequate technical supervisions are not available to obtain the ultimate loads; and
3. design the products using the given formulae for ultimate capacity.

For products which are exposed to humidity and increased water content, a 20% strength reduction should be considered.

4.2.1 Safe Loading Capacity for Veneer Panels

The uniform linear failure load w_1 can be calculated as follows:

$$w_1 = \frac{8M_{cr}}{L^2} \qquad (4.17)$$

The failure load per unit area can be derived by dividing equation (4.17) by the width b. Equation (4.17) can be written as:

$$w = \frac{8M_{cr}}{L^2 b} \tag{4.18}$$

After substituting the expression for M_{cr} from equation 4.12, the following formula can be established:

$$w_{uv} = \frac{f_{tm} h^2}{L^2}\left[2.336 + \frac{5.336 h_d}{h}\left(\frac{f_{tol} - f_{tm}}{f_{tm}}\right) - \frac{8 h_d d_{asb}}{h^2}\left(\frac{f_{tol} - f_{tm}}{f_{tm}}\right)\right] \tag{4.19}$$

With a factor of safety of S = 2.3 for a dry condition, and panel production is under factory controlled conditions, the allowable load is given as:

$$w_{avd} = \frac{f_{tm} h^2}{L^2}\left[1.015 + \frac{2.320 h_d}{h}\left(\frac{f_{tol} - f_{tm}}{f_{tm}}\right) - \frac{3.478 h_d d_{asb}}{h^2}\left(\frac{f_{tol} - f_{tm}}{f_{tm}}\right)\right] \tag{4.20}$$

For wet conditions, there is a 20% strength reduction, equation (4.20) becomes:

$$w_{avd} = \frac{f_{tm} h^2}{L^2}\left[0.812 + \frac{1.856 h_d}{h}\left(\frac{f_{tol} - f_{tm}}{f_{tm}}\right) - \frac{2.782 h_d d_{asb}}{h^2}\left(\frac{f_{tol} - f_{tm}}{f_{tm}}\right)\right] \tag{4.21}$$

Figure 4.7 shows the ultimate and allowable strength diagram in terms of load vs. span, and which was developed based on equations (4.19) and (4.20).

4.2.2 Safe Loading Capacity for Granite Pavers

Derivation similar to that of veneer panel for failure load per unit area W can be obtained using equations (4.17) and (4.18). The final expression is given as:

$$w_{up} = \frac{f_{tot} h^2}{L^2}\left[2.336 + \frac{5.336 h_{d_1}}{h}\left[\frac{f_{tol} - f_{tot}}{f_{tot}}\right] - \frac{8 h_{d_1} d'_{asb}}{h^2}\left[\frac{f_{tol} - f_{tot}}{f_{tot}}\right]\right] \quad (4.22)$$

and the allowable load for dry conditions (S = 2.3) is given as:

$$w_{apd} = \frac{f_{tot} h^2}{L^2}\left[1.015 + \frac{2.320 h_{d_1}}{h}\left[\frac{f_{tol} - f_{tot}}{f_{tot}}\right] - \frac{3.478 h_{d_1} d'_{asb}}{h^2}\left[\frac{f_{tol} - f_{tot}}{f_{tot}}\right]\right] \quad (4.23)$$

For wet conditions, equation (4.23) becomes,

$$w_{apw} = \frac{f_{tot} h^2}{L^2}\left[0.812 + \frac{1.856 h_{d_1}}{h}\left[\frac{f_{tol} - f_{tot}}{f_{tot}}\right] - \frac{2.782 h_{d_1} d'_{asb}}{h^2}\left[\frac{f_{tol} - f_{tot}}{f_{tot}}\right]\right] \quad (4.24)$$

Figure 4.8 shows the ultimate and allowable strength diagram in terms of load vs. span for granite paver supported at four corners.

4.3 Bearing Capacity of Veneer Panels

Failure loads of veneer panels subjected to compression can be calculated using the empirical equation 14.1 of section 14.2.3 of the American Concrete Institute, ACI 318 - 83 code of practice [14]. The formula gives the ultimate bearing capacity of a wall, under axial compression as:

$$P_u = 0.55 \phi f'_c A_g \left[1 - \left(\frac{k l_c}{32h}\right)^2\right] \quad (4.25)$$

Equation (4.17) should be modified if it is to take into account the presence of an asbestos - cement layer in the sandwich panels as follows:

$$P_u = 0.55\phi A_m f_{cm}[1+ m\rho][1 - (\frac{kl_c}{32h})^2] \quad (4.26)$$

where,

$$m = \frac{f_{ca}}{f_{cm}} \qquad \rho = \frac{A_{asb}}{A_m}$$

Considering the nominal bearing capacity as $P_n = P_u/\phi$, equation (4.18) can be rewritten as:

$$P_n = 0.55A_m f_{cm}[1+ m\rho][1 - (\frac{kl_c}{32h})^2] \quad (4.27)$$

A comparison of calculated nominal failure loads with test results are shown in Table 4.4.

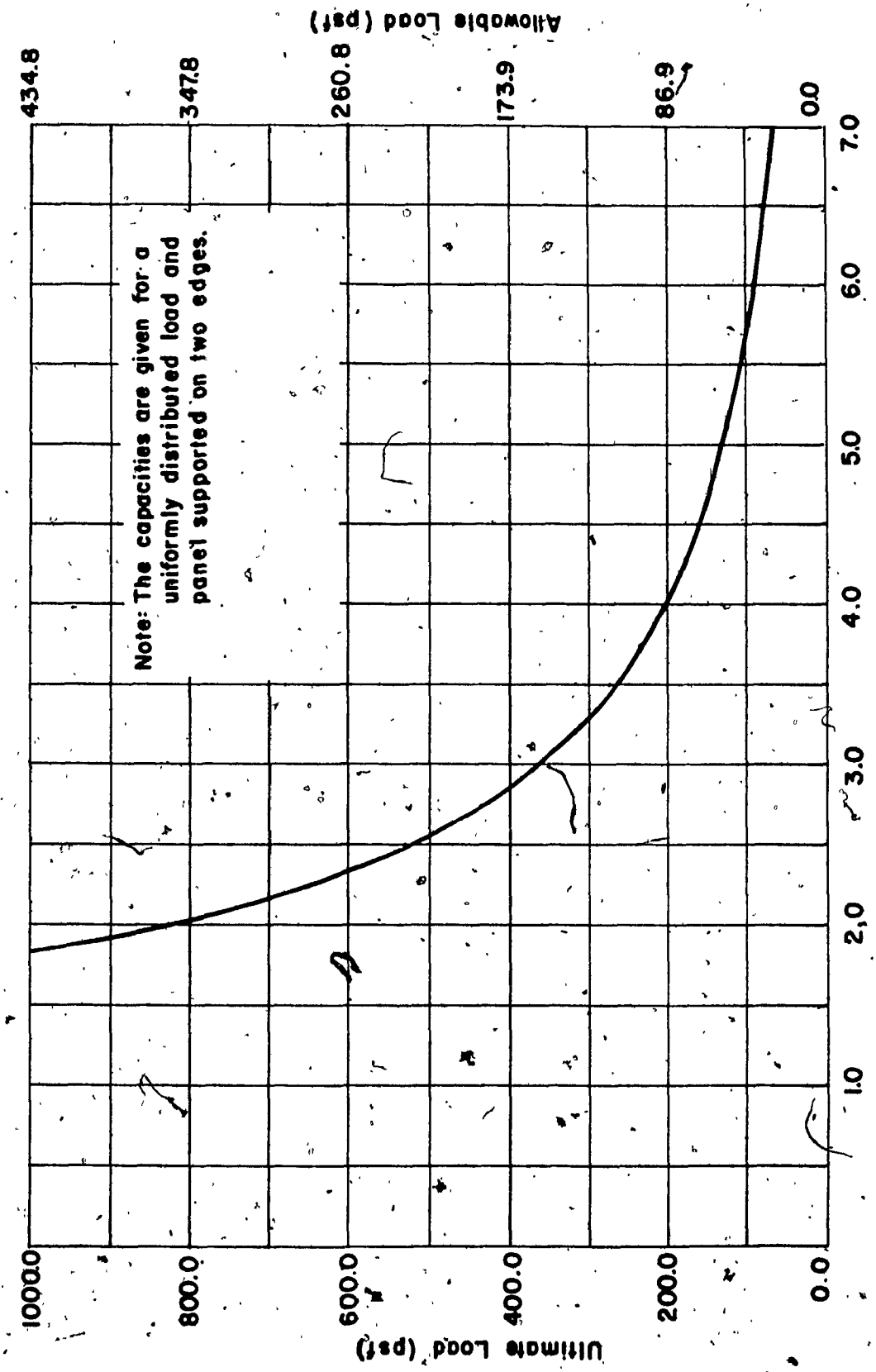

Figure 4.7 Strength diagram for veneer panels in terms of load vs. span developed based on equations (4.19) and (4.20)

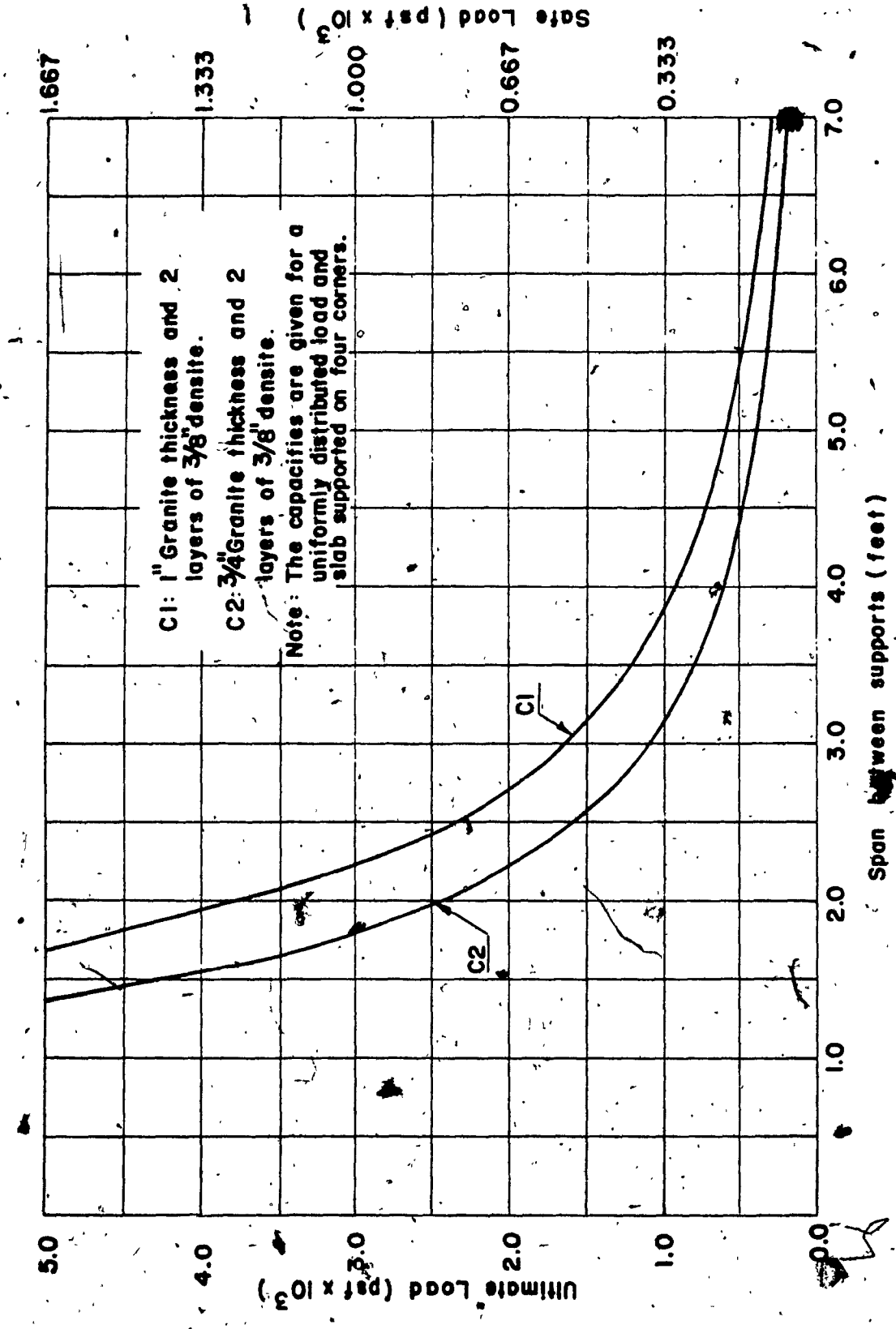

Figure 4.8 Strength diagram for granite pavers in terms of load vs. span developed based on equations (4.22) and (4.23)

$\gamma = t'_h$ / ψ_c	A				B			
	0	0.5	1.0	3	0	0.5	1.0	3
0	0.290	0.425	0.450	0.490	0.670	0.835	0.890	0.950
0.1	0.290	0.400	0.430	0.440	0.670	0.810	0.860	0.910
0.2	0.290	0.375	0.395	0.405	0.670	0.780	0.825	0.865
0.3	0.290	0.350	0.360	0.365	0.670	0.760	0.790	0.825

Table 4.1 The 'A' and 'B' coefficients for flexural cracking moment calculations

Test Series	Sample No.	Tested Failure Load (kips)	Equivalent Ultimate Uniform Load (tested) (lbs/sq.ft)	Equivalent Ultimate Uniform Load (calculated) (lbs/sq.ft)	Allowable Uniform Load (calculated for dry condition) (lbs/sq.ft)
B1	BMC1/TP I	0.300	26.48	31.37	13.64
	BMC2/TP I	0.320	27.57	31.37	13.64
	BMC1/TP II	0.520	38.55	35.00	15.22
	BMC2/TP II	0.450	34.71	35.00	15.22
	BMC3/TP II	0.390	31.42	35.00	15.22
B2	BMCN1/TP I	1.056	115.99	125.46	54.55
	BMCN2/TP I	1.010	110.94	125.46	54.55
	BMCN3/TP I	1.186	154.70	176.92	76.92
B4	BMSN1 TP II	0.997	260.68	199.37	86.68
	BMSN2/TP II	0.922	240.52	199.37	86.68
	BMSN3/TP II	0.925	241.30	199.37	86.68

Table 4.2 Comparison of calculated and test recorded flexural capacities for veneer panels

Sample No.	Tested Failure Load (kips)	Equivalent Ultimate Uniform Load (tested) (lbs/sq.ft)	Equivalent Ultimate Uniform Load (calculated) (lbs/sq.ft)	Allowable Uniform Load (calculated for dry condition) (lbs/sq.ft)
I-GP1	17.951	2371	2043	681
I-GP2	14.012	1853	2043	681
I-GP3	16.957	2242	2043	681

Table 4.3 Comparison of calculated and test recorded flexural capacities for granite pavers

Sample No.	Tested Failure Loads 'F' (kips)	Nominal Bearing Capacity 'P_n' (kips)	$\phi = \frac{F}{P_n}$
BMW1/TPII	18.658	20.250	0.92
BMW2/TPII	22.515	20.250	1.11

Table 4.4 Comparison of calculated nominal failure loads with test results for compressive bearing capacity tests

CHAPTER V

SUMMARY AND CONCLUSIONS

5.1 Summary of the Work

The present work is the first attempt in North America to study and evaluate the strength of sandwich systems with asbestos - cement sheet used to produce increased tensile strength of natural stone products. The study emphasized on developing a simple analysis method for calculating the flexural capacity of natural stone composites such as veneer panels and granite pavers which are manufactured in Canada by Atlas Turner Inc. and Bumaco.

The experimental work was conducted on full scale specimens. A total number of thirty tests were conducted. Mechanical properties of asbestos - cement and building stone materials were specified by Bumaco and Atlas Turner Inc.

A practical analysis method was developed for predicting the flexural cracking strength of veneer panels and granite pavers. The development was based on the knowledge of the stress-strain relationship of the tensioned asbestos - cement and on an assumed stress distribution at the cracking stage. The application of the empirical formula (section 14.2.3 of ACI 318 - 83) for the ultimate compressive bearing capacity of concrete walls was verified for veneer panels.

Guidelines for estimating the flexural capacity of veneer panels and granite pavers together with the bearing capacity of veneer panels have been outlined and illustrated by a practical design example shown in Appendices A, B, and C.

5.2 Conclusions

On the basis of the work described, the following conclusions are drawn:

1. The flexural capacities of veneer panels and granite paver in the reversed direction (marble or granite being at the bottom tension side) are 30% and 31% of the capacities in the normal direction (marble or granite being at the top compression zone) respectively. This observation demonstrates that the introduction of one or two layers of asbestos - cement densite in these sandwich panels is of significant improvement in comparison with solid marble or granite used in conventional settings. This sandwich combination with asbestos - cement on the tension side allows the construction of panels of larger span and loading capacity, and lesser sensitivity to breakages during transportation.

2. The results obtained from the flexural tests indicated that the proposed analysis method which is based on the non-linear stress distribution at cracking can be used to calculate the flexural capacity of the composite panels. A safety factor of 2.3 to 2.50 have been recommended. For panels exposed to high humidity or increased water content, a 20% strength reduction should be considered. Also, the design charts of Figures 4.7 and 4.8 which gives the capacity of the composite panels at different span lengths can be recommended for design practice.

3. The bond strength between each different layer of material was sufficient and did not affect the overall capacity of the composite panels.

4. The strength of veneer panels subjected to compression can be calculated according to the present ACI practice for wall design (ACI 318 - 83). However, the validity of this conclusion is influenced by the critical parameter $kl_c/32h$. The limit for this parameter is:

$$\frac{kl_c}{32h} < 1.0$$

REFERENCES

1. American Society for Testing and Materials. "Standard Methods of Conducting Strength Tests of Panels for Building Construction (Designation: E72 - 80)". Annual Book of ASTM Standards, Vol. 04.07, pp. 282 - 297. Philadelphia: ASTM, 1983.
2. American Society for Testing and Materials. "Standard Method of Measuring Relative Resistance of Wall, Floor, and Roof Construction to Impact Loading (Designation: E695 - 79)". Annual Book of ASTM Standards, Vol. 04.07, pp. 701 - 705. Philadelphia: ASTM, 1983.
3. American Society for Testing and Materials. "Standard Test Method for Performance of Wood and Wood - Based Floor and Roof Sheathing Under Concentrated Static and Impact Loads (Designation: E661-79)". Annual Book of ASTM Standards, Vol. 04.07, pp. 663 - 671. Philadelphia: ASTM, 1984.
4. De - Mahieu, L., "La Theorie de L'Asbeste - Ciment", S. A. Eternit N. V., Kapell - Op - Den - Bos, p. 359j, Belgium, 1973.
5. Murashev, V. I., "Cracking Resistance, Stiffness and Strength of Reinforced Concrete", Mashstroiizadi, 268 pp., Moscow, 1950. (In Russian).
6. Mourachev, V., Sigalov, E. and Baikov, V., Constructions en Béton Armé, pp. 224 - 226, Moscow, 1971.
7. Perinayegon, A., "Tests and Strength Evaluation of Asbestos - Cement Housing Structures", M. Eng Thesis, p. 95, Concordia University, Montreal, 1984.
8. Zielinski, Z. A., and Zampino, G. P., "Report on the Testing of Asbestos-Cement 'U' Facade Panels", Report #3, p. 51, Concordia University, Montreal, 1984.
9. Allen, H. G., "The Purpose and Methods of Fibre Reinforcement", Prospect for Fibre Reinforced Construction Material, Proceedings of an International Building Exhibition Conference Sponsored by the Building Research Station, Olympia, pp. 3 - 14, London, 1971.

10. Sigalov, E., and Strongin, S. Reinforced Concrete, p. 160, Gordon and Breach Science Publishers, Inc., New York, 1963.

11. Bljuger, F. "Cracking Resistance of Concrete Members in Bending". ACI Journal, Proceedings V. 82, No. 4, pp. 467 - 474, July - August 1985.

12. Aveston, J., Mercer, R. A., and Sillwood, J. M. "Fibre Reinforced Cements - Scientific Foundations for Specifications". Composites Standards Testing and Design. Conference Proceedings of Physical Laboratory, IPC Science and Technology Press, pp. 104 - 105, London, 8 - 9 April 1974.

13. Swamy, R.N., and Kameswara Rao, C.V.S. "Some Engineering Considerations of Fibre Concrete", Composites Standards Testing and Design. Conference Proceedings of Physical Laboratory, IPC Science and Technology Press, pp. '04 - 105, London, 8 - 9 April 1974.

14. ACI Committee 318, "Building Code Requirements for Reinforced Concrete (ACI 318 - 83)", American Concrete Institute, Detroit, 1983.

15. Logan, D. and Shah, S. P., "Moment Capacity and Cracking Behaviour of Ferrocement in Flexure", ACI Journal, Proceedings V. 70, No. 12, pp. 799 - 804, December 1973.

16. Chang, W. F. et al., "Flexural Behaviour of Ferrocement Panels", American Society of Civil Engineers Ocean Engineering Conference, Civil Engineering in the Oceans, Vol. II, pp. 1023 - 1044, December, 1969.

17. Tancreto, J. E. and Haynes, H. H., "Flexural Strength of Ferrocement Panels", Tech. Report R. 772, Naval Civil Eng. Lab, Port Hueneme, California, August, 1972.

18. Aagren, P. and Harrison, N. L., "Strength of Concrete Beams and Pipes at First Crack - A Strain Limit Design Method", ACI Journal, Proceedings V. 83, No. 1, pp. 156 - 161, Jan - Feb 1986.

APPENDIX A

CALCULATION EXAMPLES OF FLEXURAL CAPACITY OF VENEER PANELS

Panels BMC1/TPII - BMC3/TPII (Densite at the bottom)

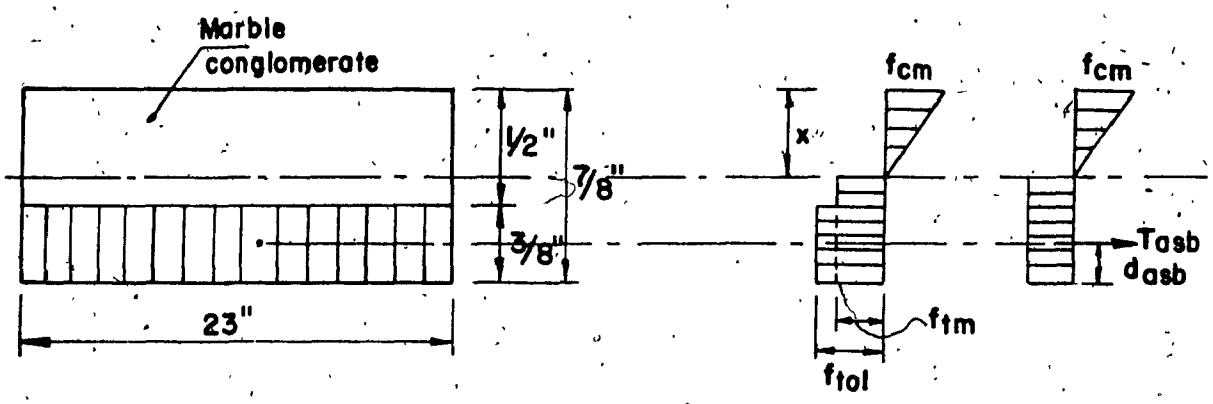

Geometric Properties of the Cross - Section:

b = 23"

h = 7/8" = 0.875"

A_{asb} = 23 x 3/8 = 8.625 in^2

Material Properties:

f_{tol} = 2100 psi

f_{rmarb} = 2030 psi

f_{tm} = 2030 ÷ 1.75 = 1160 psi (ψ = 1.75 for rectangular section)

The Coefficients of Strengthening of Section:

$$\psi_t = \frac{A_{asb}\,(f_{tol} - f_{tm})}{bhf_{tm}}$$

$$= \frac{8.625\,(2100 - 1160)}{(23)(0.875)(1160)} = 0.347$$

$$\psi_c = 0; \quad \gamma = \frac{t'}{h} = \frac{0}{7/8} = 0$$

Location of Neutral Axis at Cracking Stage:

$$\frac{x}{h} = \frac{1 + \Psi_t}{2 + 2\Psi_c + \Psi_t}$$

$$\frac{x}{(0.875)} = \frac{1 + 0.347}{2 + 2(0) + 0.347}$$

$$x = 0.5"$$

$$A = 0.5 - \left[\frac{0(0)}{1 + 2(0)}\right] - \left[\frac{1 - 2(0)}{6(1 + 2(0)}\right] - \frac{1}{6}\left[\frac{1 + 2(0)}{2 + 2(0)}\right]^2$$

$$= 0.292$$

$$B = 1 - \left[\frac{0(0)}{1 + 2(0)}\right] - \left[\frac{1}{3(1 + 2(0))}\right] = 0.667$$

$$\Sigma\Psi_{ti}\,\delta_i = \frac{(23)(0.375)(0.1875)(2100 - 1160)}{(23)(0.875)^2(1160)} = 0.074$$

$$M_{cr} = f_{tm}\, bh^2\, [A + B\Psi_t - \Sigma\Psi_{ti}\,\delta_i]$$

$$= (1160)(23)(0.875)^2\,[0.292 + 0.667(0.347) - (0.074)]$$

$$= 9171 \text{ lbs - in.}$$

and the corresponding tested value was Mcr = 9055 lbs-in. (average)

$$M_{cr} = \frac{wL^2}{8}$$

$$w = \frac{8M_{cr}}{L^2} = \frac{8(9171)}{(114)^2} = 5.65 \text{ lbs/in.}$$

$$\therefore \text{ Ultimate load per unit area} = \frac{5.65}{23} = 0.245 \text{ lbs/in}^2 = 35 \text{ psf.}$$

APPENDIX B

CALCULATION EXAMPLE OF FLEXURAL CAPACITY OF GRANITE PAVER

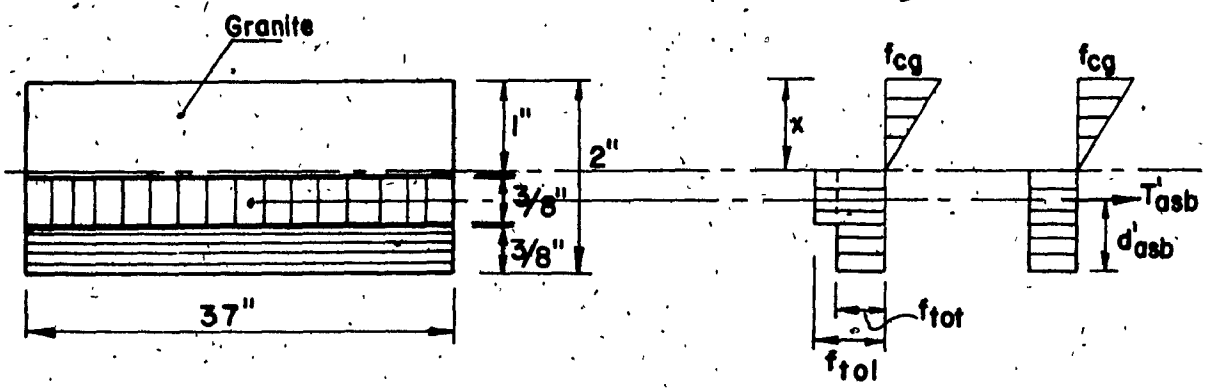

Geometric Properties of Cross - Section:

b = 37"

h = 2"

A_{asb2} = 37 x 3/8 = 13.875 in^2

Material Properties:

f_{tot} = 1450 psi

f_{tol} = 2220 psi

The Coefficients of Strengthening of Section:

$$\psi_t = \frac{A_{asb2}[f_{tol} - f_{tot}]}{bhf_{tot}}$$

$$= \frac{(13.875)(2220 - 1450)}{(37)(2)(1450)} = 0.0996$$

$$\psi_c = 0; \quad \gamma = \frac{t'}{h} = \frac{0}{2} = 0$$

Location of Neutral Axis at Cracking Stage:

$$\frac{x}{h} = \frac{1 + \psi_t}{2 + 2\psi_c + \psi_t}$$

$$\frac{x}{2} = \frac{1 + 0.0996}{2 + 2(0) + 0.0996}$$

$$x = 1.05"$$

$$A = 0.5 - \left[\frac{0(0)}{1 + 2(0)}\right] - \left[\frac{1 - 2(0)}{6(1 + 2(0)}\right] - \frac{1}{6}\left[\frac{1 + 2(0)}{2 + 2(0)}\right]^2$$

$$= 0.292$$

$$B = 1 - \left[\frac{0(0)}{1 + 2(0)}\right] - \left[\frac{1}{3(1 + 2(0))}\right] = 0.667$$

$$\Sigma\psi_{ti}\ \delta_i = \frac{(37)(0.375)(0.5)(2220 - 1450)}{(37)(2)^2(1450)} = 0.0249$$

$$M_{cr} = f_{tot}\, bh^2\, [A + B\psi_t - \Sigma\psi_{ti}\ \delta_i]$$

$$= (1450)(37)(2)^2\, [0.292 + 0.667(0.0996) - (0.0249)]$$

$$= 71461.8 \text{ lbs - in.}$$

and the corresponding tested value was 75386.1 lbs-in. (average).

$$M_{cr} = \frac{w L^2}{8}$$

$$w = \frac{8M_{cr}}{L^2} = \frac{8(71461.8)}{(33)^2} = 525 \text{ lbs/in.}$$

$$\therefore \text{ Ultimate load per unit area } = \frac{w}{b} = \frac{525}{37} = 14.2 \text{ lbs/in.}^2 = 2043 \text{ psf.}$$

APPENDIX C

BEARING CAPACITY CALCULATION FOR VENEER PANELS

Panels BMW1/TPII - BMW2/TPII

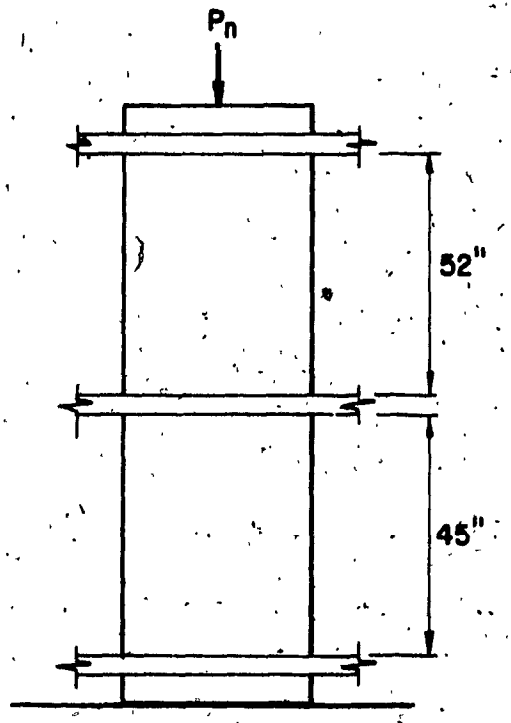

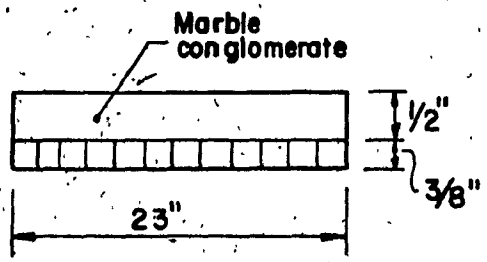

SECTION

Geometric Properties of the Cross.- Section:

b = 23"

h = 0.875"

A_{asb} = 3/8 x 23 = 8.625 in^2

A_m = 1/2 x 23 = 11.5 in^2

Material Properties

f_{ca} = 8600 psi

f_{cm} = 16795 psi

Coefficients for Calculations:

$$m = \frac{f_{ca}}{f_{cm}} = \frac{8\,600}{16\,795} = 0.512$$

$$= \frac{A_{asb}}{A_m} = \frac{8.625}{11.5} = 0.75$$

k = 0.5 for fixed supports

l_c = 52"

$$P = 0.55 A_m f_{cm} [\,1 + m\rho\,] [\,1 - \left[\frac{kl_c}{32h}\right]^2\,]$$

$$= 0.55(11.5)(16\,795)\,[\,1 + (0.512)(0.75)\,]\,[\,1 - \left[\frac{0.5(52)}{32(0.875)}\right]^2\,]$$

$$= 20\,252 \text{ lbs.} \cong 20.25 \text{ kips}$$

Ultimate bearing capacity per linear feet $= \frac{20.25}{23} \times 12 = 10.56$ k/ft.

and the corresponding tested value was 20.58 kips (average).